

NASA TM-77005

NASA TECHNICAL MEMORANDUM

NASA TM-77005

CONSTRUCTION AND TEST OF FLEXIBLE WALLS FOR THE THROAT  
OF THE ILR HIGH-SPEED WIND TUNNEL

Yukihiro Igeta

NASA-TM-77005 19830010500

Translation of "Konstruktion und Erprobung von Flexiblen Wänden für die Messtrecke des ILR-Hochgeschwindigkeits-Windkanals," Institute for Aerodynamics and Aeronautics, Technische Universität, Berlin, West Germany, Report, Sept. 1978, pp 1-57

APR 11 1983

FEB 2 1983

LANGLEY RESEARCH CENTER  
LIBRARY, NASA  
HAMPTON, VIRGINIA

NATIONAL AERONAUTICS AND SPACE ADMINISTRATION

WASHINGTON, D.C. 20546 FEBRUARY 1983



NF00287

## STANDARD TITLE PAGE

1. Report No. NASA TM-77005	2. Government Accession No.	3. Recipient's Catalog No.	
4. Title and Subtitle CONSTRUCTION AND TEST OF FLEXIBLE WALLS FOR THE THROAT OF THE ILR HIGH-SPEED WIND TUNNEL.		5. Report Date FEBRUARY 1983	
		6. Performing Organization Code	
7. Author(s) Yukihiro Igeta, Institute for Aerodynamics and Aeronautics, Technical University, West-Berlin, Germany (West)		8. Performing Organization Report No.	
		10. Work Unit No.	
9. Performing Organization Name and Address Leo Kanner Associates, Redwood City, CA. 94063		11. Contract or Grant No. NASw-3541	
		13. Type of Report and Period Covered Translation	
12. Sponsoring Agency Name and Address National Aeronautics and Space Administration, Washington, D.C. 20546		14. Sponsoring Agency Code	
15. Supplementary Notes Translation of "Konstruktion und Erprobung von Flexiblen Wänden für die Messtrecke des ILR-Hochgeschwindigkeits-Windkanals," Institute for Aerodynamics and Aeronautics, Technische Universität, Berlin, West Germany, Report, Sept. 1978, pp 1-57			
16. Abstract Aerodynamic tests in wind tunnels are jeopardized by the lateral limitations of the throat. This influence expands with increasing size of the model in proportion to the cross-section of the throat. Wall interferences of this type can be avoided by giving the wall the form of a stream surface that would be identical to the one observed during free flight. To solve this problem, flexible walls that can adapt to every contour of surface flow are needed.			
17. Key Words (Selected by Author(s))		18. Distribution Statement Unlimited	
19. Security Classif. (of this report) Unclassified	20. Security Classif. (of this page) Unclassified	21. No. of Pages	22.

N83-18771#  
N-153,517

Mr. Yukihiro Igeta, Matr. no. A4877

TOPIC

/2\*

Construction and Test of Flexible Walls for the Throat  
of the ILR High-Speed Wind Tunnel

Abstract

Aerodynamic tests in wind tunnels are jeopardized by the lateral limitations of the throat. This influence increases with increasing size of the model with respect to the cross-section of the throat. Wall interferences of this type can be prevented by shaping the wall as a stream surface identical to the one observed during free flight. To solve this problem, flexible wind-tunnel walls are needed which can assume any contour of surface flow.

Literature:

1. Goodyer, M.J.: "A low speed self streamlining wind tunnel. Windtunnel design and testing techniques." AGARD-CP-174, 1975.
2. Chevallier, J.P.: Parois autocorrectrices pour soufflerie transsonique [Self-correcting walls for a transsonic wind tunnel] 12<sup>ème</sup> Colloque d'aérodynamique appliquée. ENSMA/CEAT Poitiers Nov. 5-7, 1975.

Problem Statement:

Within the frame of this study, a windtunnel throat is to be designed for the installation of flexible walls. The starting point for the design is an existing throat of the ILR. The design drawings are to be prepared according to workshop specifications.

For the flexible walls of the throat including the pertinent adjusting mechanisms, a preliminary design shall be produced.

---

\*Numbers in the margin refer to pagination in the foreign language document.

The proposal can be based on the theoretically determined flow-line profiles for a NACA 0012 airfoil, which give an idea of the wall deflections and curvatures expected in practice.

Based on the preliminary design, a model shall be prepared for testing of various wall materials and of the adjusting mechanism. This testing shall determine the anticipated adjusting tolerances for various numbers of adjusting elements and shall show which arrangement proves to be most favorable.

Based on the experiences gained in this test series, a proposal shall be made for the final design of the flexible windtunnel walls.

Prof. Uwe Ganzer, Ph.D.

Institut fuer Luft- und Raumfahrt (ILR)  
Technische Universitaet, Berlin

TABLE OF CONTENTS	Page
List of Symbols	vi
1. Introduction	1
2. Windtunnel Throat	2
2.1 Selection of Materials	2
2.2 Design of the Throat Housing	3
2.3 Calculation of the Housing Stress	4
2.4 Determination of the Housing-plate Thickness	5
2.5 Rough Calculations of the Load Capacity of the Components	6
2.5.1 Side Wall	7
2.5.2 View Window	8
2.5.3 Cover and Base Plate	9
2.5.4 Circular Plate	9
3. The Flexible Walls of the Throat	10
3.1 Flow Profile of the NACA 0012 Airfoil	10
3.2 Number and Location of Wall Supports	11
3.3 Wall Materials for the Flexible Wall	12
3.4 Wall Adjusting Mechanism	15
3.5 Test Set-up for the Flexible Wall	15
3.6 Measurement of Wall Contour Deviation	15
3.7 Evaluation of the Measured Results	16
4. Summary	17
Bibliography	19
Figures and Tables	20

## List of Symbols

E	Elasticity modulus
F	Surface area
I	Polar moment of inertia
K	Plate stiffness
M	Mach number
$P_0$	Pressure at rest
T	Temperature
h	Plate thickness
m	Moment relative to one unit of cut length
w	Sag
$\sigma_{zul}$	Allowable stress
$\sigma_{0.2}$	Elastic limit

# Construction and Test of Flexible Walls for the Throat of the ILR High-Speed Wind Tunnel

Yukihiro Igeta

Institute for Aerodynamics and Aeronautics  
Technical University  
Berlin, West Germany

## 1. Introduction

/2

Aerodynamic investigations in wind tunnels are jeopardized due to the limited expansion of the air stream. A rigid throat causes the flow lines to be compressed about the model. However, free-flowing edges cause an expansion of the flow lines. This effect on the flow field leads to a falsification of measured results in the windtunnel.

In the case of fixed windtunnel walls, a wall interference can only be prevented when the throat walls are far enough away from the model that the disturbance of the flow caused by the model has diminished before reaching the wall. This requires large windtunnels whose energy consumption is inordinately high.

Another solution is a throat with flexible walls, where the throat walls have precisely the shape of the flow surface, which would be present at this point in a flow field of infinite size.

Chevallier [1] and Goodyer [2] have successfully used such throats with flexible walls for two-dimensional flow studies. The result shows a good approximation of the pressure distribution of an airfoil to that of the interference-free case.

In this study, a windtunnel throat with flexible wall is to be proposed. In order to do this, various wall materials will be tested and the adjusting mechanism and its location will be tested in a separate test set-up.

## 2. Windtunnel Throat

### 2.1 Selection of Materials

The starting point for the design of the windtunnel throat was the dimension of the throat of the ILR high-speed windtunnel:

$$\text{Height: } h = 156 \text{ mm}$$

$$\text{Width: } b = 150 \text{ mm}$$

$$\text{Length: } l = 700 \text{ mm}$$

For reasons of weight saving and easy manipulation, the aluminum alloy type AlCuMg was selected as material; this material is also used in aircraft construction.

The specific weight  $\gamma$  alone is not determinative for the total weight. The permissible stresses and the elasticity modulus of the material are primarily responsible in this case. They are related by a characteristic factor K.

The components of the housing are subjected to bending stress due to the underpressure in the throat. The factor for parts subjected to bending stress, measured with respect to load capacity ( $K_T$ ) and rigidity of shape ( $K_F$ ) are [3]:

$$K_T = \frac{\gamma}{\sqrt[3]{\sigma_{zul}^2}} \quad K_F = \frac{\gamma}{\sqrt{E}}$$

For aluminum alloy, it follows:

$$K_T = 14,7 \cdot 10^{-3} \frac{\sqrt[3]{N}}{\sqrt[3]{cm^5}} \quad \text{and} \quad K_F = 1,0 \cdot 10^{-3} \frac{\sqrt{N}}{cm^2}$$

$$\text{with } \begin{aligned} \gamma &= 0,027 \frac{N}{cm^3} \\ E &= 700 \frac{N}{cm^2} \\ \sigma_{zul} &= 2,5 \frac{N}{cm^2} \end{aligned}$$

For steel (construction steel St42) we have:

$$K_T = 42,3 \cdot 10^{-3} \frac{\sqrt[3]{N}}{\sqrt[3]{cm^5}} \quad \text{and} \quad K_F = 1,7 \cdot 10^{-3} \frac{\sqrt{N}}{cm^2}$$



$$\begin{aligned} \text{with } \gamma &= 0,078 \frac{N}{cm^2} \\ E &= 2100 \frac{N}{cm^2} \\ \sigma_{\text{zul}} &= 2,5 \frac{N}{cm^2} \end{aligned}$$

The values for aluminum alloy are clearly lower.

## 2.2 Design of the Throat Housing

The throat housing consists in principle of 6 main parts:

- 2 side walls
- 1 cover plate
- 1 base plate
- 1 nozzle flange
- 1 diffuser flange

These parts are screwed together into a throat housing and sealant is applied to the joints (fig.1). The two flexible walls are installed into the housing as upper and lower throat limiters. The two spaces resulting above and below the flexible walls are connected with the throat. Thus, the same static pressure results in the two spaces as in the throat flow. The flexible walls and their adjusting parts are thus not under stress and this is intended to prevent sagging of the flexible walls between the individual adjusting parts.

A view window of acrylic glass (polymethacrylic acid methyl ester) is installed in a side wall to permit observation of the deformation of the flexible walls. The opposite side wall has a circular disc for holding the airfoil.

The airfoil NACA 0012 is screwed eccentrically to the disc by two bolts. The radius of the circular disc is sized so that during a change in setting angle, a vertical shift of the airfoil occurs simultaneously from the throat midline. This assures that the stagnation flow line is found in the middle of the upper and lower flexible wall in an adjusting-angle range of about  $-15^{\circ}$  to  $-15^{\circ}$  (fig. 1). /5

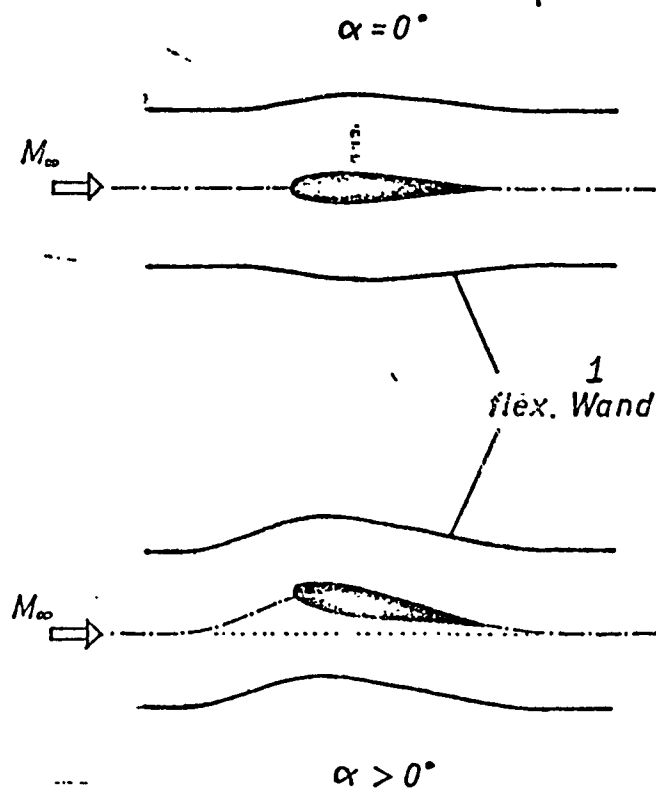


Figure 1. Key: 1-flexible wall

### 2.3 Calculation of the Housing Stress

/6

The throat housing is stressed by the underpressure in the throat. The calculation of the static pressure in the flow results from the equation for a compressible, frictionless flow:

$$\frac{P_0}{P} = \left[ 1 + \frac{\alpha-1}{2} M^2 \right]^{\frac{\alpha}{\alpha-1}}$$

With the blower-stream mach number of  $M_{\max} = 0.9$  and  $\alpha = 1.4$  for air, we have:  $\frac{P_0}{P} = 1.52$

$P_0 = 10332 \frac{\text{kp}}{\text{m}^2} \hat{=} 101.4 \cdot 10^3 \frac{\text{N}}{\text{m}^2}$  in an ICAO standard atmosphere at  $H=0\text{m}$  and  $T=288\text{K}$

$$\Rightarrow P = 66.5 \cdot 10^3 \frac{\text{N}}{\text{m}^2}$$

From the external pressure  $P_0 = 101.4 \cdot 10^3 \frac{\text{N}}{\text{m}^2}$  and the static pressure

in the housing, there results the pressure difference  $\Delta P$ :

$$\Delta P = P_0 - p = 1014 \cdot 10^3 \frac{N}{m^2} - 66,5 \cdot 10^3 \frac{N}{m^2}$$

$$\Delta P = 35 \cdot 10^3 \frac{N}{m^2}$$

## 2.4 Determination of the Housing-plate Thickness

The thickness of the housing plate must be sufficient so that the plate undergoes the smallest possible deformation under load. A maximum wall deformation of 0.1 mm - 0.2 mm would not affect the flow quality in the throat.

For a determination of this thickness, the solution to the plate equation for freely-rotating, universally supported plates [4] was used.

From:

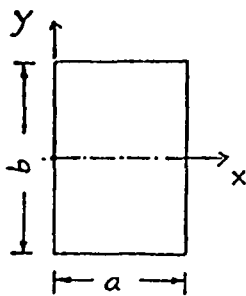
$$\frac{\partial^4 w}{\partial x^4} + 2 \frac{\partial^2 w}{\partial x^2 \partial y^2} + \frac{\partial^4 w}{\partial y^4} = \frac{p}{K}$$

$$\Delta \Delta w = \frac{p}{K}$$

there follows the sag for a uniformly-distributed full load:

$$w = \frac{4p a^4}{K \pi^5} \sum_n \frac{1}{n^5} \left\{ 1 - \frac{1}{2 \cosh \frac{\alpha_n b}{2}} \left[ \left( 2 + \frac{\alpha_n b}{2} \operatorname{tgh} \frac{\alpha_n b}{2} \cdot \right. \right. \right. \quad /7$$

$$\left. \left. \left. \cdot \cosh \alpha_n y - \alpha_n y \sinh \alpha_n y \right] \right\} \sin \alpha_n x \quad (1.0)$$



with:  $n = 1, 3, 5 \dots$

$$\alpha_n = \frac{n \cdot \pi}{a}$$

$$K = \frac{E \cdot h^3}{12(1-\mu^2)}$$

$p$ : surface-area load  $\cong \Delta P$

This series converges very quickly (n=1). For the plate midpoint  $x = \frac{1}{2}a$ ,  $y=0$ , we have:

$$w_{\max} = \frac{4 p a^4}{K \pi^5} \left\{ 1 - \frac{1}{2 \cosh \frac{\pi b}{2a}} \left( 2 + \frac{\pi b}{2a} \operatorname{tgh} \frac{\pi b}{2a} \right) \right\} \quad (1.1)$$

Solved for the plate thickness:

$$h^3 = \frac{48 p a^4 (1-\mu^2)}{E \pi^5 w_{\max}} \left\{ 1 - \frac{1}{2 \cosh \frac{\pi b}{2a}} \left( 2 + \frac{\pi b}{2a} \operatorname{tgh} \frac{\pi b}{2a} \right) \right\}$$

With the dimensions of the side wall:  $a = 400$  mm;  $b = 650$  mm, the value of the E-modulus and the transverse contraction ratio:

$$E = 72 \cdot 10^3 \frac{N}{m^2}$$

$$\mu = 0.34$$

we have the plate height  $h = 22$  mm, where  $w_{\max} = 0.1$  mm was used for the maximum sag.

A plate thickness of 20 mm was selected. The calculation with this plate thickness gives a max. sag of  $w_{\max} = 0.14$  mm. This value is not attained in practice since the plate is stressed in the housing on all sides. For example, the ratio of the sag of fixed beam to hinged beam is:

$$\frac{w_{\text{fixed}}}{w_{\text{hinged}}} = 0.25$$

and that of fixed to hinged quadratic plates is:

$$\frac{w_{\text{fixed}}}{w_{\text{hinged}}} = 0.3$$

## 2.5 Rough Calculations of the Load Capacity of the Components

The rough calculations of the load capacity of the individual components is done without formation of comparison stresses--for the sake of simplicity--by means of which the multiaxis stress state is converted back into a monoaxis one.

### 2.5.1 Side Wall

The greatest bending moment in the middle of the plate is computed from the equation for freely-rotating rectangular plates:

$$m_x = \frac{4\rho a^2}{\pi^3} \sum_n \frac{1}{n^3} \left[ 1 - \frac{1-\mu}{2 \cosh \frac{\alpha_n b}{2}} \left( \frac{2}{1-\mu} + \frac{\alpha_n b}{2} \tanh \frac{\alpha_n b}{2} \right) \right] \quad (1.2)$$

$$\text{with } \alpha_n = \frac{n\pi}{a}$$

For	$n = 1$	$\Rightarrow m_{x1} = 522 \text{ N}$
	$n = 3$	$m_{x3} = -26,6 \text{ N}$
	$n = 5$	$m_{x5} = 5,8 \text{ N}$
	$n = 7$	$m_{x7} = -2,1 \text{ N}$
	$n = 9$	$m_{x9} = 1,0 \text{ N}$
	$n = 11$	$m_{x11} = -0,6 \text{ N}$

$$m_{\max} = \sum_{i=1}^{11} m_{xi} = 499,5 \text{ N} \approx 500 \text{ N}$$

From the equations

$$\sigma_x = - \frac{E \cdot z}{1-\mu^2} \left( \frac{\partial^2 w}{\partial x^2} + \mu \frac{\partial^2 w}{\partial y^2} \right)$$

$$m_x = -K \left( \frac{\partial^2 w}{\partial x^2} + \mu \frac{\partial^2 w}{\partial y^2} \right)$$

the stress  $\sigma_x$  can be computed:

$$\sigma_x = \frac{12 m_x}{h^3} \cdot z \quad (1.3)$$

During bending, the max. stresses occur on the edge zones; with a plate thickness of  $h=20 \text{ mm}$ , we have  $z = \pm 10 \text{ mm}$ . When substituted into the above equation:

$$\Rightarrow \sigma_{\max} = 7,5 \frac{\text{N}}{\text{mm}^2}$$

The elastic limit of aluminum alloy lies about at  $\sigma_{0,2}^t = 250 \frac{\text{N}}{\text{mm}^2}$ . The maximum stress on the stressed plate is very much smaller than the elastic limit:

$$\sigma_{\max} < \sigma_{0,2}$$

## 2.5.2 View Window

The maximum sag for the acrylic glass window results from equation (1.1):

$$w_{max} = 0.9 \text{ mm} \quad \text{with} \quad \begin{aligned} a &= 310 \text{ mm} \\ b &= 510 \text{ mm} \\ \mu &= 0,35 \\ E &= 4 \cdot 10^3 \frac{N}{mm^2} \\ h &= 20 \text{ mm} \end{aligned}$$

By gluing on two strips of acrylic glass (size: 10mm x 20mm), the view window was reinforced and divided. The sag in the middle of the window is thus decreased considerably. From the equation for a fixed, square plate, we then have the maximum sag of  $w = 0,00127 \frac{p a^4}{K}$ ,  $w_{max} = 0.14 \text{ mm}$ ; with  $a=b=310 \text{ mm}$ .

The airfoil fixed in the middle of the throat forms an additional support for the view window.

The max. bending moment on the plate without acrylic strips is derived from equation (1.2).

For	$n = 1 \Rightarrow m_{x_1} = 314 \text{ N}$
	$n = 3 \quad m_{x_3} = -11,6 \text{ N}$
	$n = 5 \quad m_{x_5} = 2,5 \text{ N}$
	$n = 7 \quad m_{x_7} = -0,9 \text{ N}$

$$m_{max} = \sum_{i=1}^7 m_{x_i} = 304 \text{ N}$$

From equation (1.3) there results for the stress:

$$\sigma_{max} = 4,6 \frac{N}{mm^2}$$

The elastic limit for the acrylic glass has the value of about:

$$\sigma_{0,2} = 70 \frac{N}{mm^2}$$

$$\Rightarrow \sigma_{max} < \sigma_{0,2}$$

### 2.5.3 Cover and Base Plate

Calculations for the cover and base plates measuring:

$a = 150 \text{ mm}$ ,  $b = 650 \text{ mm}$ ,  $h = 20 \text{ mm}$ ;  $b/a = 4.3$ .

As the ratio of  $b/a$  increases, the solution of equation (1.0) approaches the simple solution for the plate strips. When the ratio of  $b/a = 4.5$ , this result is sufficiently accurate. The solution for plate strips fixed on both sides under uniformly-distributed full load runs:

$$w(x) = \frac{\rho a^4}{384K} \left( 1 - 8 \frac{x^2}{a^2} + 16 \frac{x^4}{a^4} \right)$$

For the max. sag, we have:

$$w_{max} = w(x=0) = \frac{\rho a^4}{384K}$$

$$w_{max} = 0,86 \cdot 10^{-3} \text{ mm}, \text{ with } E = 72 \cdot 10^3 \frac{N}{\text{mm}^2} \text{ and } \mu = 0,34$$

Bending moment:

$$m(x) = - \frac{\rho a^4}{384} \left( 16 - 19,2 \frac{x^2}{a^2} \right)$$

$$m_{max} = m(x=0) = \frac{\rho a^4}{24}$$

$$m_{max} = 32,8 \text{ N}$$

Stress:

$$\text{From (1.3)} \quad \Rightarrow \quad \sigma_{max} = 0,5 \frac{N}{\text{mm}^2}$$

$$\sigma_{max} < \sigma_{0,2}$$

### 2.5.4 Circular Plate

Calculations for the circular plate (airfoil mount):

The dimensions:  $\emptyset = 2a$ ;  $a = 160 \text{ mm}$ ;  $h = 20 \text{ mm}$ .

Solution for a circular plate with a freely-rotating suspension at the edge  $r=a$  under uniformly-distributed full load:

$$w(r) = \frac{p}{64K} \left( \frac{5+\mu}{1+\mu} a^4 - 2 \frac{3+\mu}{1+\mu} a^2 r^2 + r^4 \right)$$

For the greatest sag, we have:

$$w_{\max} = w(r=0) = \frac{5+\mu}{1+\mu} \frac{p a^4}{64K}$$

$w_{\max} = 0.026$  mm, with  $E = 72 \cdot 10^3 \frac{N}{mm^2}$  and  $\mu = 0,34$ .

The bending moment from:

$$m_{\max} = (3+\mu) \frac{p a^3}{16}$$

$$m_{\max} = 56 \text{ N}$$

The stress from (1.3):

$$\Rightarrow \sigma_{\max} = 0,84 \frac{N}{mm^2}$$

$$\sigma_{\max} < \sigma_{0,2}$$

The greatest stresses occurring in the individual components are very much smaller than the elastic limit of the material.

The design drawings for the throat are found in the appendix (figures 2 to 10).

### 3. The Flexible Walls of the Throat

#### 3.1 Flow Profile of the NACA 0012 Airfoil

Theoretically determined flow-line profiles for a NACA 0012 airfoil were taken as a basis for the design of the wall-adjusting mechanism and its distribution along the throat.

With an existing computer program, based on the panel method [5], flow-line profiles with  $0^\circ$ ,  $6^\circ$  and  $10^\circ$  adjustment angle of the airfoil, were produced for the deflection range of the flexible walls between adjusted angles of  $0^\circ$  and  $10^\circ$  (fig. 11 to 13). The deflection of the wall flow-line in all three figures is about  $x/c = 0.3$ . For an investigation of the wall deformation, the flow lines of the airfoil with an adjusted angle of  $10^\circ$  were selected,



since these lines have the greatest curvature of the three settings (fig. 21).

The flow-file profile was enlarged to a 1:1 scale (profile length: 100 mm), in order to be able to measure the contour more accurately. To compute the slope and curvature of the flow-line contour, it was simulated by a spline function formed from 17 support points (table 1). The profile of the contour ( $f(x)$ ), the slope ( $f'(x)$ ) and the curvature ( $k=f''/(1+f'^2)^{3/2}$  are shown in fig. 14, since  $f'(x) \leq 0$  it follows  $k=f''(x)$ ).

### 3.2 Number and Location of Wall Supports

With increasing number of wall adjusting parts, the deviation of the flexible wall becomes smaller compared to the flow-line contour. The arrangement of wall adjusting parts must be selected so that a good approximation of the wall contour to the flow-line shape is assured with a small number of adjusting parts.

An adjusting part (5) was provided at the point of greatest deflection  $x/c = 0.35$ , so that the flexible wall attains the greatest-possible deflection of the flow line.

The environ of the inflection point ( $y' = \text{const.}$ ) can be approximated by straight lines. In order to obtain these lines, adjusting parts are needed at their end points (adjusting parts 2, 3 and 6, 7 in fig. 15). An adjusting part (1) was attached at  $x/c = -1.65$ , since at this point the curvature changes. The large difference in curvature at the adjusting parts (3) and (5) which are 70 mm apart, was bridged by an adjusting part (4) at  $x/c = 0.05$ . Between the adjusting part (7) at  $x/c = 1.65$  and (8) at  $x/c = 2.25$ , the slope of the flow-line curve is again constant. This region can be approximated by a straight wall contour.

/14

From this follows a number of 8 adjusting parts. Near the airfoil where the largest curvature occurs, there are 4 adjusting parts close together. Each pair of adjusting parts supports the

flexible wall before and behind the airfoil. The ratio of the flexible wall length to the number of adjusting parts is 7.51 cm/support. In the self-correcting windtunnel of M.J. Goodyer [2], the ratio is 7.11 cm/support and of J.P. Chevallier [1], it is 6.88 cm/support.

The irregular deviation of the computed slope and curvature values of the flow line from the actual flow line, is explained by the following reasons:

1. The input data for the support points of the spline function contain inaccuracies due to the computation.
2. The overshoot of spline curve is possible from the flow line between the support points.
3. These errors are additive when taking the derivatives.

The qualitative profile of the wall curve and its derivatives are shown in fig. 14.

### 3.3 Wall Materials for the Flexible Wall

As wall material, plastic was chosen for its elasticity, flexibility and good damping properties. But the material must have a certain stiffness so that the wall will not bend due to the resulting pressure difference between its upper and lower sides (especially near the airfoil) and due to its own weight between the supports.

Three commercial thermoplastics came into consideration:

1. Polyvinylchloride (PVC)
2. Polycarbonate (PC; trade name: Macrolon)
3. Polymethylmethacrylate (PMMA; trade name: Plexiglas)

In the table below, the mechanical properties of these plastics are presented [6]:

	PMMA	PC	PVC-hart
Zugfestigkeit $\left[\frac{\text{kp}}{\text{cm}^2}\right]$	1100 (-40°C) 800 (+23°C)	800 (-40°C) 600 (+20°C)	500-650
Reißdehnung $\left[\frac{\text{g}}{\text{g}}\right]$	5 - 6	80 - 110	20 - 50
E-Modul $\left[\frac{\text{kp}}{\text{cm}^2}\right]$	33000	20-22 · 10 <sup>3</sup>	30-34 · 10 <sup>3</sup>
Biegefestigk. $\left[\frac{\text{kp}}{\text{cm}^2}\right]$	1400		
Grenz - " - $\left[\frac{\text{kp}}{\text{cm}^2}\right]$		900	750-1100
Schlag- zähigkeit $\left[\frac{\text{cmkp}}{\text{cm}^2}\right]$	12 (20°C) ca 10 (-60°C)	ohne (20°C) Br. (-100°C)	ohne Bruch
Kerbschlag- zähigkeit $\left[\frac{\text{cmkp}}{\text{cm}^2}\right]$	ca 2	20-30(+20°C) 10-15(-40°C)	2-3(+20°C) 2-2,5(-20°C)
Kriechmodul b. 23°C (Prüfspann. 200 $\frac{\text{kp}}{\text{cm}}$ )	1h: 29000 100h: 25000	1h: 20000 100h: 18000	1h: 32000 100h: 30000

Key: 1-tensile strength 2-elongation at break 3-E-modulus  
4-bending resistance 5-strength limit 6-impact resistance  
7-notched-bead resistance 8-creep modulus at 23 °C (test stress 200 kp/cm) 9-no break

PMMA: Hard, stiff, does not fragment on break. Good tensile, compression and tensile strength and low deformation, generally scratch-resistant.

PVC-hard: Hard, stiff, may chip (impact resistant PVC types are less sensitive), high strength. Brittle at -5 °C, impact-resistant types to -25 °C.

PC: High strength and high hardness with good toughness; very good shape retention with low temperature dependence up to 140 °C. Good impact resistance. Favorable creep strength over time, even at high temperatures. Brittle below -190 °C [7].

The flexible wall will be installed into a throat where the temperature varies, depending on mach number, between the outside temperature (at M = 0) and -25 °C (at M = 0.9). It is expected that another temperature will prevail on the flow side of the flexible wall due to the presence of the boundary layer, than that on the side turned toward the adjusting mechanism. The plastic

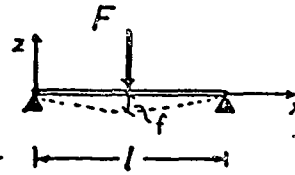
"polycarbonate" has good mechanical properties even at low temperatures.

With the equations for hinged beams with single load:

$$F = \frac{48 \cdot E \cdot I}{l^3} \cdot f$$

$$M_{max} = \frac{F \cdot l}{4}$$

$$\sigma = \frac{M}{J} \cdot z$$



it follows for the sag f:

$$f_{max} = \frac{l^2}{12z} \cdot \frac{\sigma_{max}}{E}$$

For the three plastics (PMMA, PC, PVC) with the same dimensions, we have:

$$f_{max} = konst. \cdot \frac{\sigma_{max}}{E}$$

$$f_{max} \sim \frac{\sigma_{max}}{E}$$

Substituted for the three plastic's tensile strength and E-modulus:

$$PMMA: \quad f \sim \frac{950 \frac{kp}{cm^2}}{33000 \frac{kp}{cm^2}} = 0.029$$

$$PC: \quad f \sim \frac{700 \frac{kp}{cm^2}}{21000 \frac{kp}{cm^2}} = 0.033$$

$$PVC: \quad f \sim \frac{575 \frac{kp}{cm^2}}{32000 \frac{kp}{cm^2}} = 0.018$$

Polycarbonate has the largest sag value. PC has the greatest flexure of the three wall materials.

In order to keep the load on the wall-adjusting parts as small as possible during the deformation of the wall, but also to have a certain wall stiffness, a wall thickness of 2 mm was selected for the test set-up.

### 3.4 Wall Adjusting Mechanism

The flexible wall is first provided manually with a spindle. The adjusting mechanism is shown in fig. 16. A grooved ball bearing of small size is used to absorb the rotary motion of the spindle, because the force generated by the deformation of the wall is very small (max. 100 N).

The 2 articulated joints one above the other are needed in order to offset the shift of the wall suspension-point during wall deformation and at the same time, to permit a variable wall slope at this point.

### 3.5 Test Set-up for the Flexible Wall

A test set-up was prepared with 4 adjusting parts (fig. 17) in order to test the adjusting mechanism and to investigate the deviation of the wall contour from the flow line with this reduced number of adjusting elements.

A half-frame of plywood was used as support for the flexible wall. The fixed bearing of the wall is illustrated in fig. 18, whereas fig. 19 shows the shifting bearing of the wall on the diffuser side.

### 3.6 Measurement of Wall Contour Deviation

From the profile of flow lines at the positions of the adjusting parts, the particular deflection was determined and adjusted on the wall. On the mid-line of the deformed wall the wall deflection was measured by a dial gauge at 19 points and compared with the flow line contour. Figure 20 shows the used combinations of number and location of adjusting elements. In these tests, only the combinations were selected with which the greatest deflection of the flow line contour was attained. In this manner the number of measurements was reduced. The deviations of the wall contour from the flow-line contour are shown in figures 22 to 25.

### 3.7 Evaluation of the Measured Results

To determine the adjusting tolerances of flexible walls, we investigated a wall with 4 adjusting parts as an example. The investigation should show what number and location of adjusting elements are needed in order not to exceed a specific wall adjusting tolerance.

The evaluation of the measured results shows that for a wall-contour setting, an adjusting-element arrangement can be found so that a specified, small wall deviation is attained with a minimum of adjusting parts. For example, it is possible to obtain a smaller deviation of the wall contour with two favorably-located adjusting parts, than with three or four adjusting parts. But if the best arrangement of the adjusting parts is selected, then with increasing numbers of adjusting elements, smaller wall-adjusting tolerances result (fig. 26).

The smallest measured wall-contour deviation with four adjusting parts, shown in fig. 26, is larger than those with two and three adjusting parts. The reason for this lies in the selection of the location of the adjusting elements made at the beginning of the test. Through the addition of an additional adjusting element 2 at  $x/c = -1.15$  to the combination F with three adjusting parts 4, 5 and 6 (fig. 25), the value of the smallest wall-adjusting tolerance would be reduced with four adjusting parts to  $|\Delta y| = 0.3$  mm (⊙-symbol in fig. 26).

The measured results (fig. 22-25) show that the front part of the flow-line contour ( $y' > 0$ ) can also be approximated sufficiently by the wall without intermediate support ( $|\Delta y| < 0.7$  mm). The front region of the flow line contour has a constant curvature and slope, in contrast to the rear region. For this reason, the wall-adjusting tolerance in the front region is less with a smaller number of adjusting parts.

A deviation in wall contour with 8 adjusting parts can be estimated through combination of curves A and B in fig. 22. In the region of adjusting parts 4 and 5 however, the estimation is inaccurate due to the combination of the two curves. On the other hand, the error due to the closely-packed adjusting parts cannot become large. Over the entire wall length, the max. wall-contour deviation is  $|\Delta y| = 0.2 \text{ mm}$ ). This error is on the same order as that of the material production tolerances.

Thus with 8 adjusting elements, a good approximation of the wall to the flow-line contour can be achieved with sufficient wall stiffness. When reducing the number of adjusting elements, the flexible wall must be reinforced in the flow direction. But this causes the adjusting forces to become large during the deformation of the wall.

In table 2 the measured results of three wall materials are presented for the same number and arrangement of adjusting elements. For a specified wall contour which is to be put in place by the adjusting parts, the deformation of the flexible wall is independent of the wall materials. The different elasticity modulus is expressed only in different support forces for the adjusting parts. A comparison of measured values of the three wall materials PMMA, PC, PVC confirms this theoretical state of affairs. The deviations lie within the tolerance for wall production.

The manual adjusting mechanism can be taken over for future applications, except for a few changes to the back wall-mount (fig. 27). A suggestion for a wall adjustment with an electric motor is illustrated in fig. 28.

#### 4. Summary

An aluminum alloy was selected for the throat structure in order to save weight and to assure easy handling. The wall adjustment can be observed through a large plexiglas window. The adjusting-angle setting of the airfoil takes place via a circular disc

attached eccentrically to the profile.

For the wall deformation the investigation of the flow-line profile of a NACA 0012-airfoil gives an arrangement with 8 adjusting parts. As wall material, the Polycarbonate plastic was chosen due to its good mechanical properties and flexibility.

The measured results with 4 adjusting parts show that an arrangement of adjusting elements can be found for a wall-contour setting where a small wall deviation is attained with a minimum number of adjusting parts. Through combination of two measured curves each with 4 adjusting parts, a wall contour deviation with 8 adjusting elements can be estimated. The maximum deviation  $|\Delta y| = 0.2$  mm applies over the entire wall length. With 8 adjusting elements, a good approximation of the wall to the flow-line contour could be achieved with sufficient wall stiffness.

An investigation of the influence of the wall-contour deviation on the flow field will be left for the windtunnel testing.



## REFERENCES

1. Chevallier, J.P.: "Parois autocorrectrices pour soufflerie transsonique." [Self-correcting walls for a transsonic wind tunnel] 12ème Colloque d'aérodynamique appliquée. ENSMA/CEAT Poitiers 5-7 Nov. 1975.
2. Goodyer, M.J.: "A Low-Speed, Self-Streamlining Wind tunnel", Wind tunnel design and testing Techniques, AGARD-CP-174, 1975.
3. Tochtermann/Bodenstein: "Konstruktionselemente des Maschinenbaues" [Construction Elements of Mechanical Engineering] Part 1.
4. Girkmann, K.: "Flächentragwerke" [Wing Assemblies].
5. Rosch, H.: "Analyse der Langsamflugeigenschaften von Transonikprofilen. Studienarbeit" [Analysis of Slow Flight Characteristics of Super Sonic Airfoils; A Study].
6. Carlowitz: "Kunststoff-Tabellen" [Plastics Tables].
7. Hellerich: "Werkstoff-Führer Kunststoff" [Materials Guide to Plastics].

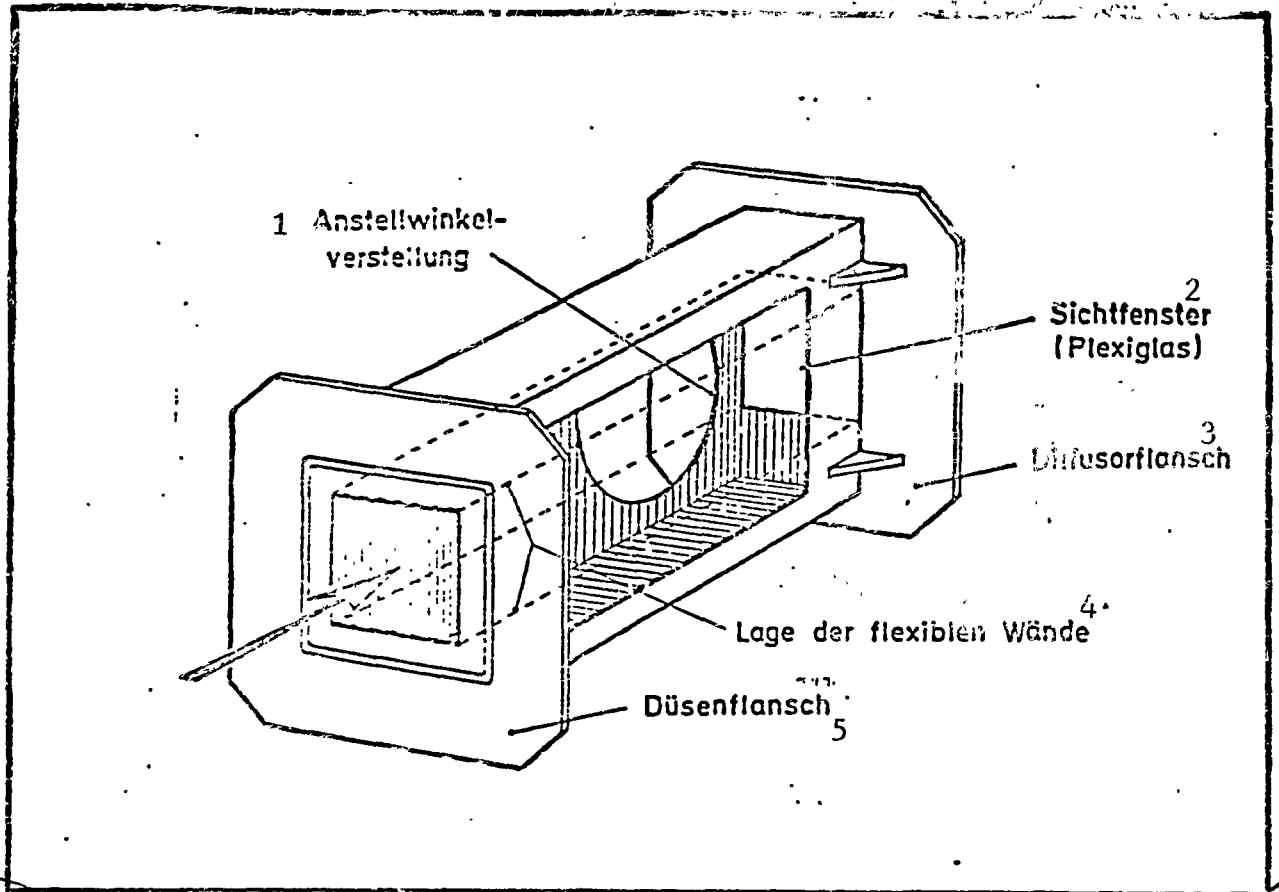


Figure 1: Throat Housing

Key: 1-setting of adjusting angle 2-view window (plexiglass)  
 3-diffuser flange 4-location of the flexible walls  
 5-nozzle flange

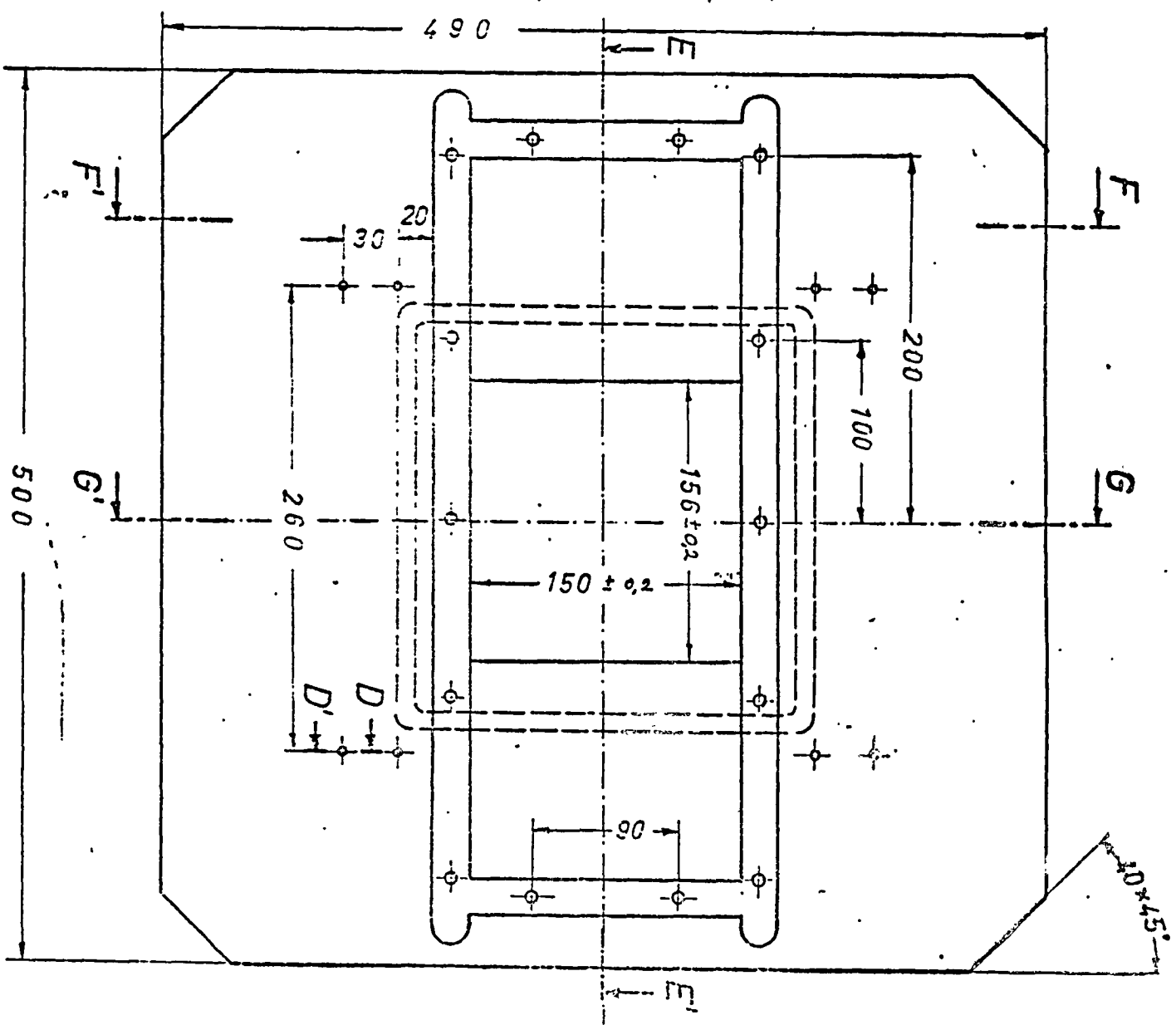
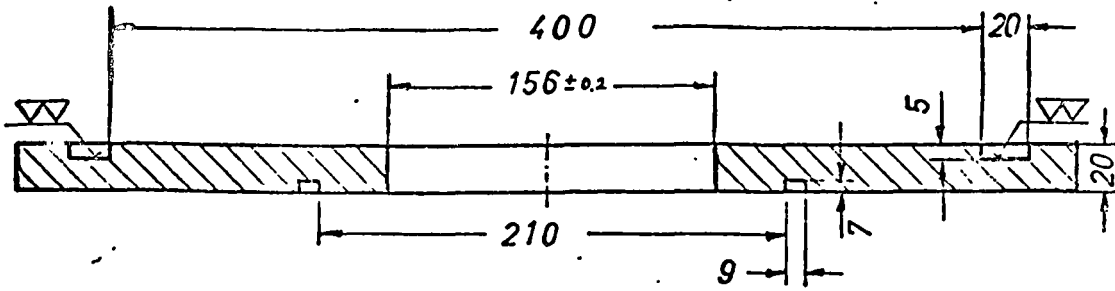


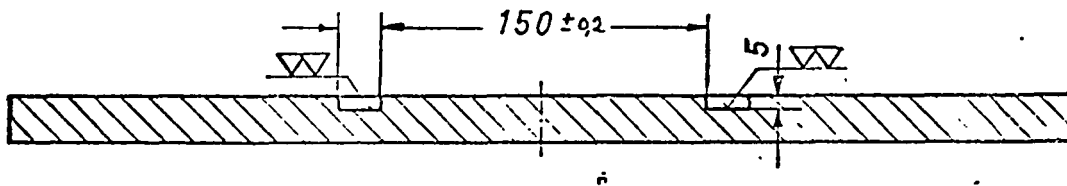
Figure 2: Flange

Scale 1:3

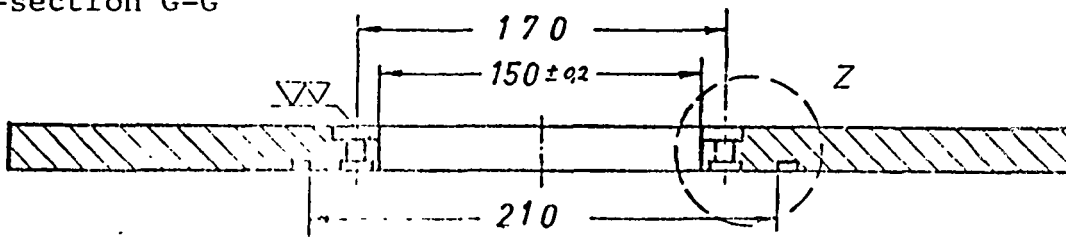
Cross-section E-E'



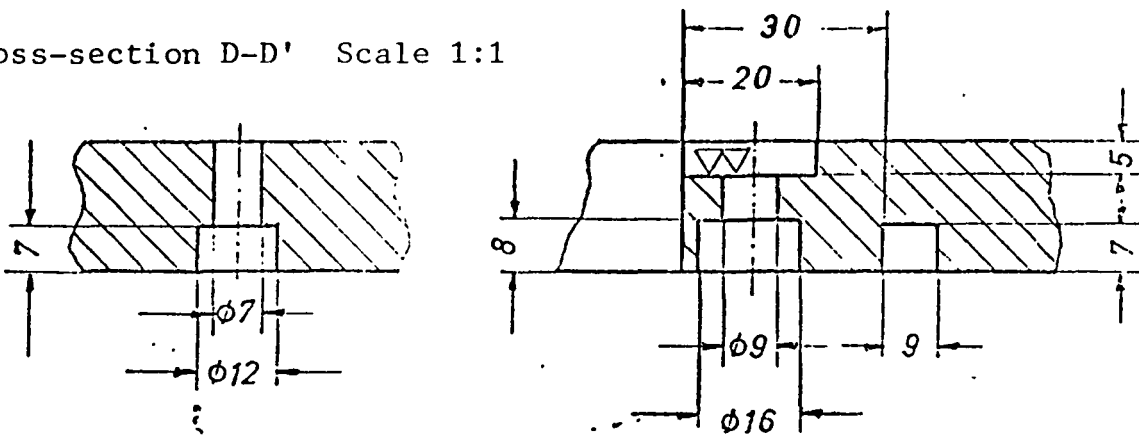
Cross-section F-F'



Cross-section G-G'



Cross-section D-D' Scale 1:1



Detail Z Scale 1:1

Figure 3

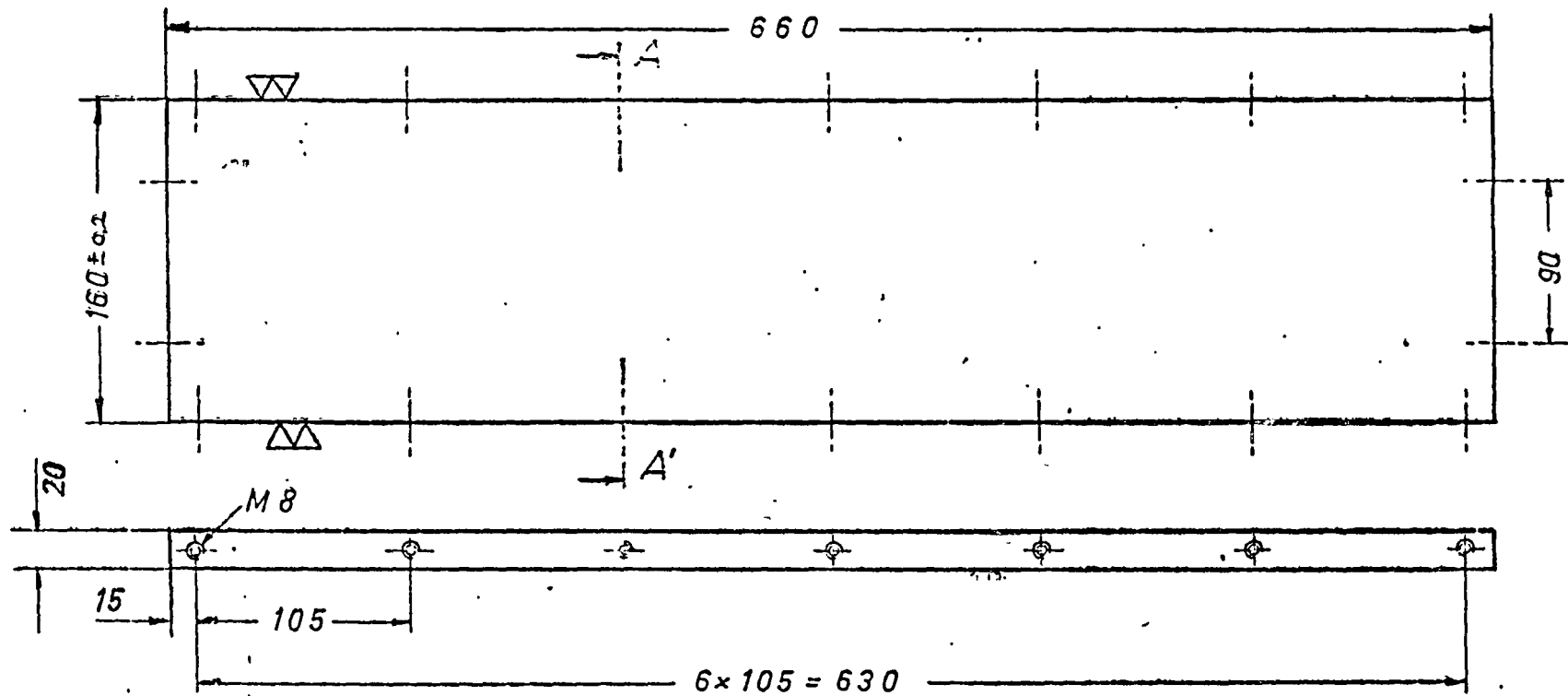
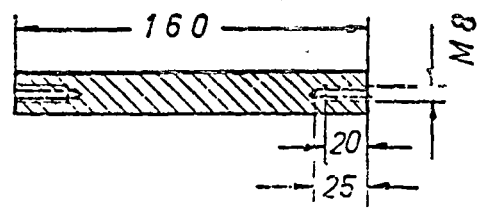


Figure 4

Section A-A'



Cover and Base Plate  
Scale 1:3

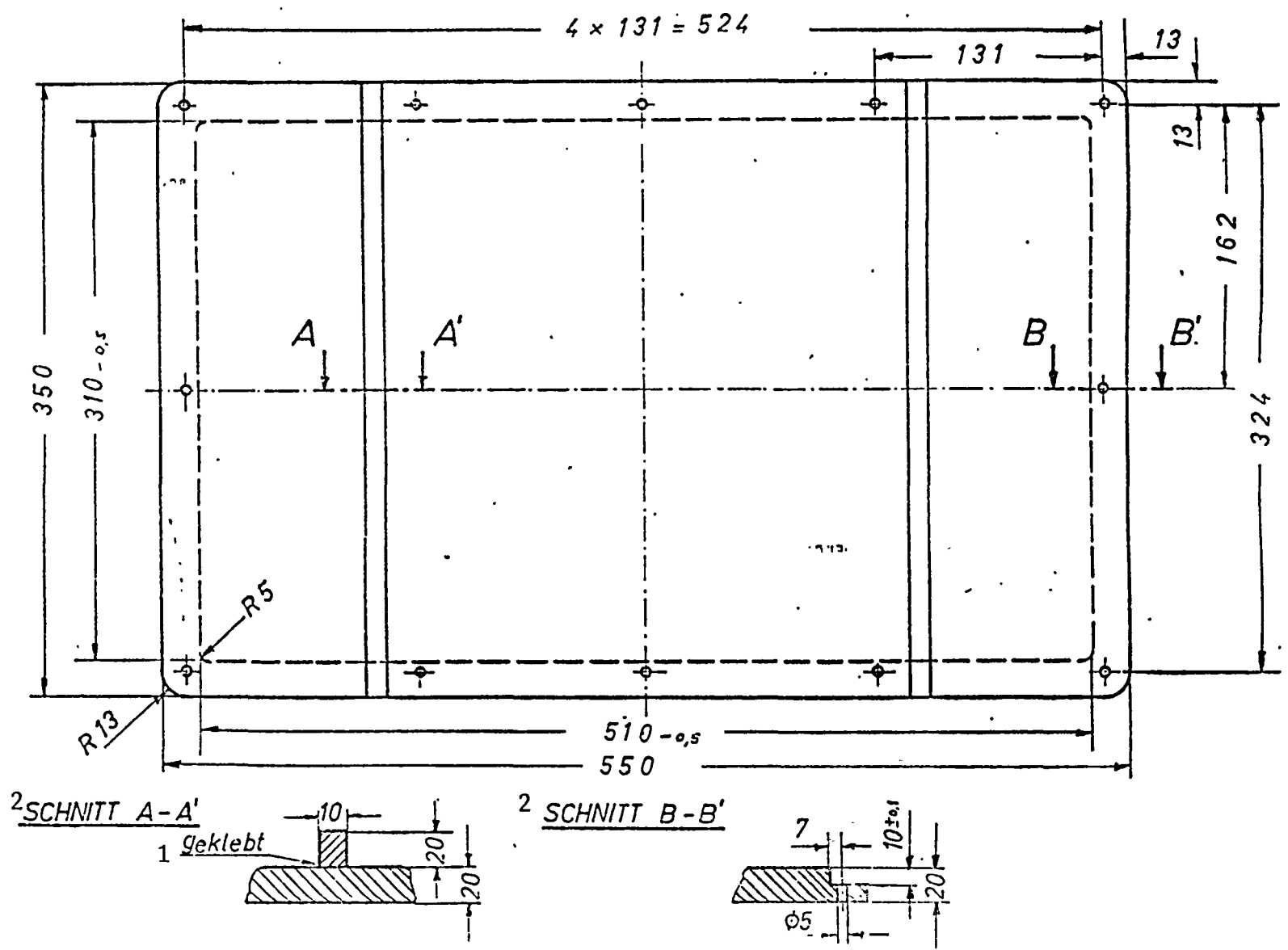


Figure 5: PMMA Window. Scale: 1:3

Key: 1-glued 2-cross-section

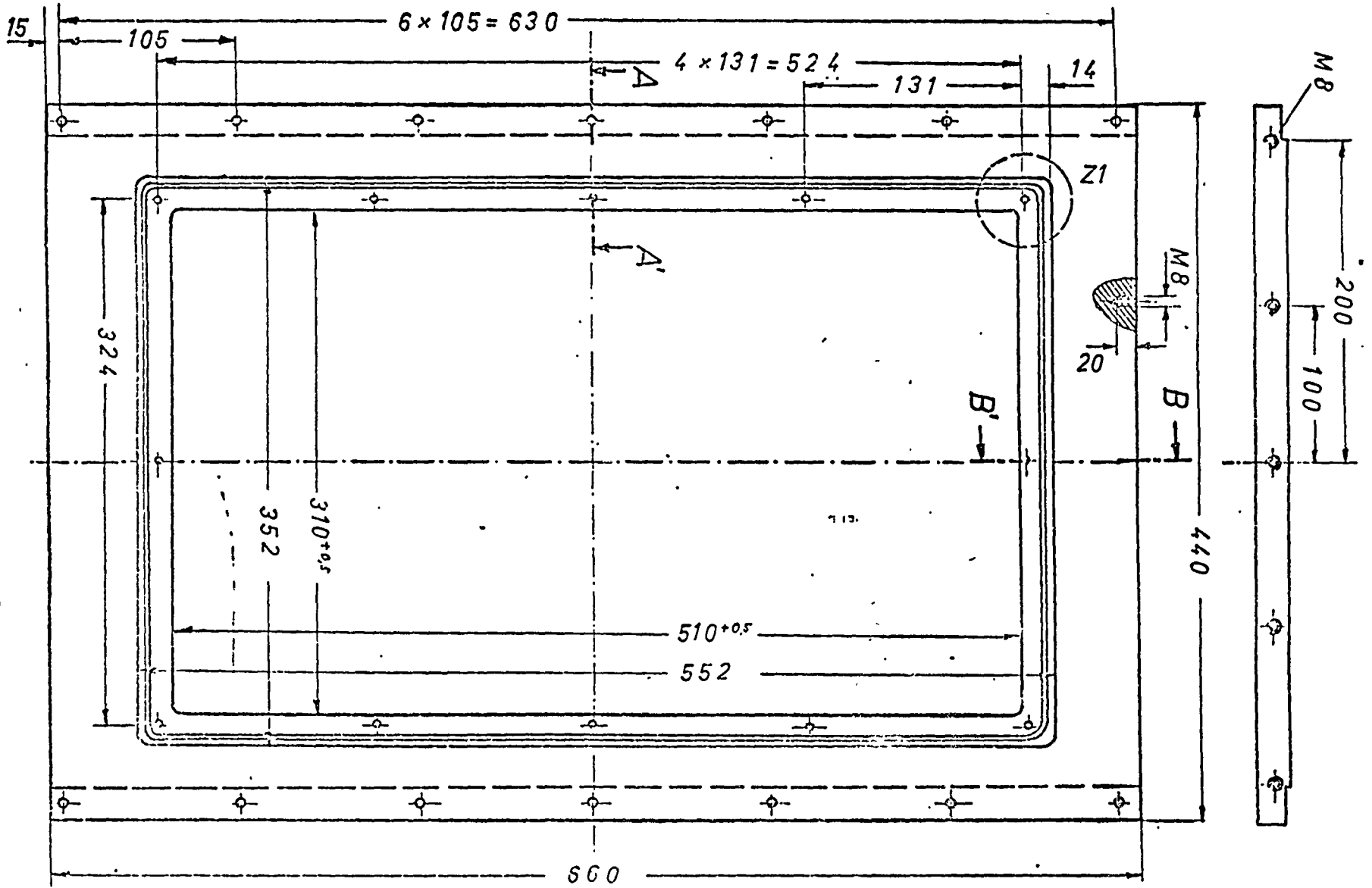
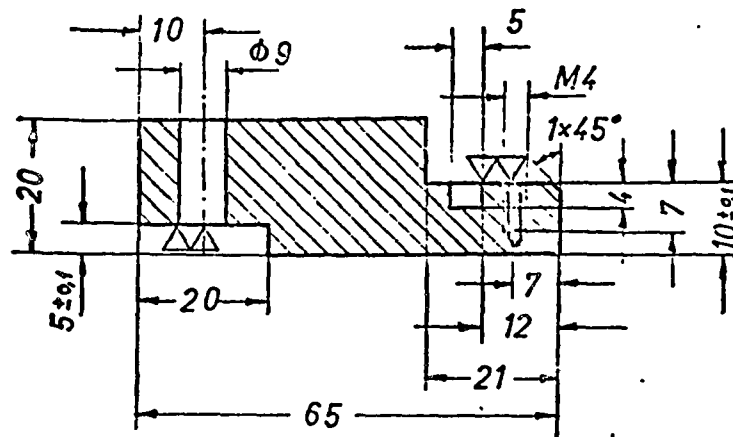
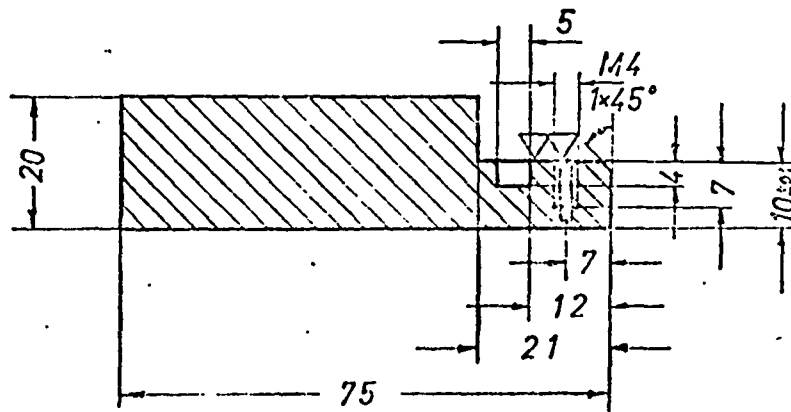


Figure 6. Side Wall; Scale 1:3

Cross-section A-A'



Cross-section B-B'



Detail Z1

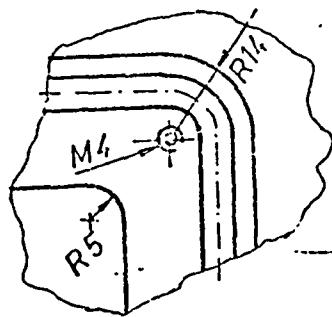
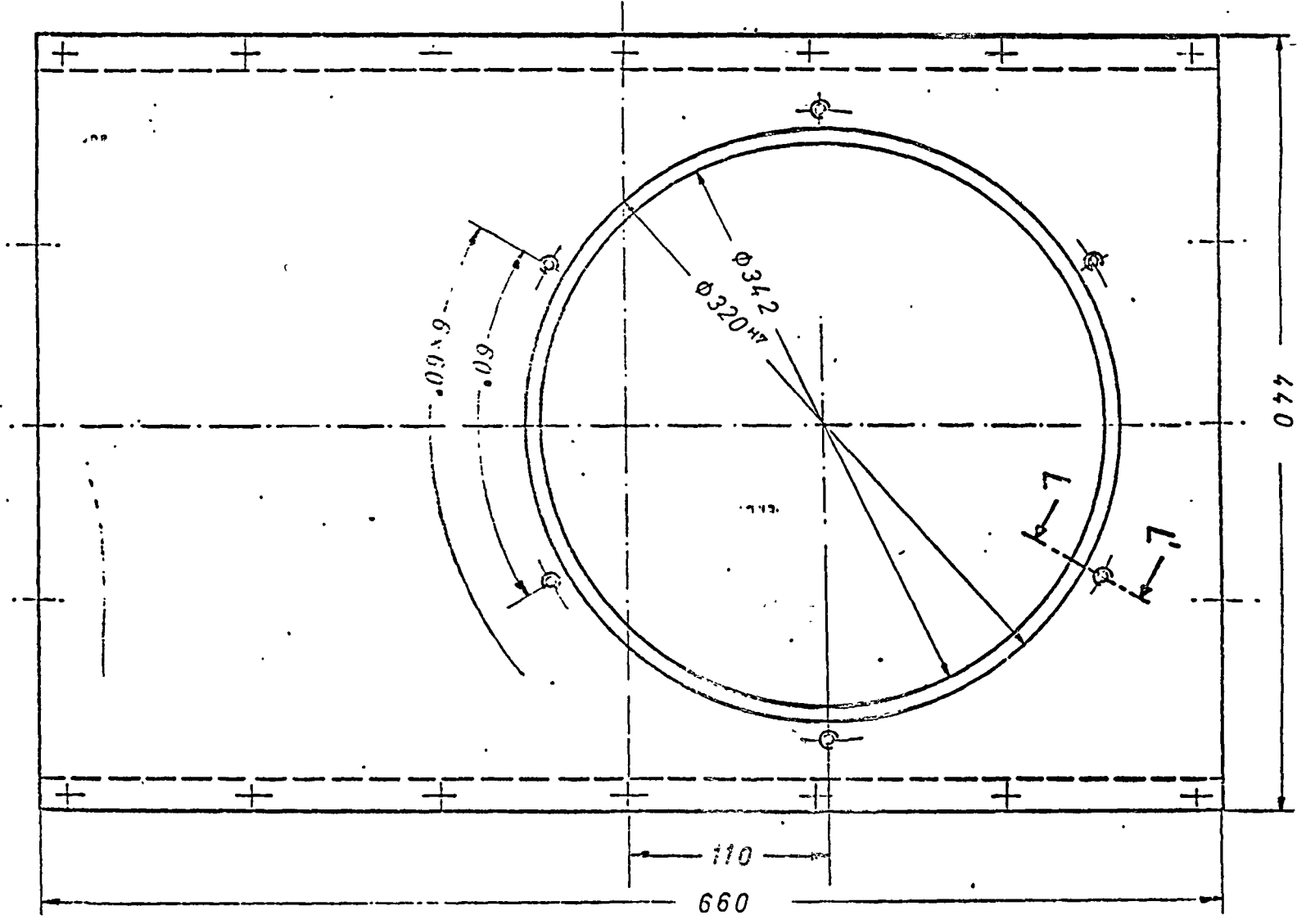
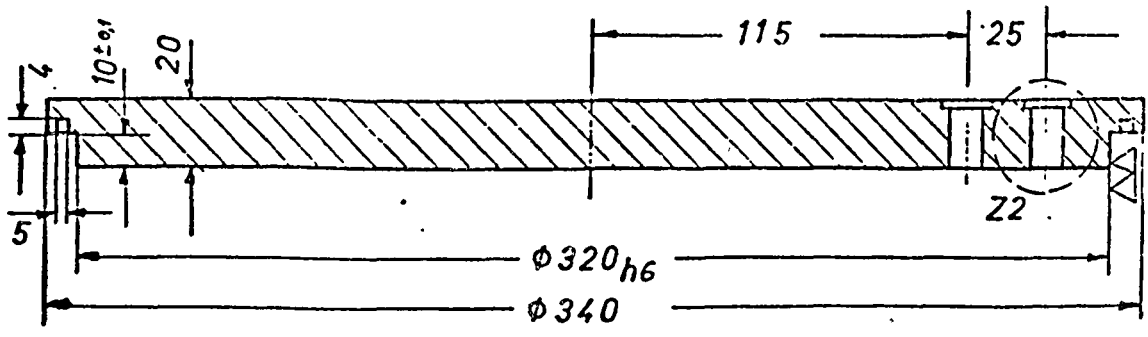


Figure 7



Figure 8: Side Wall; Scale 1:3





Cross-section K-K'

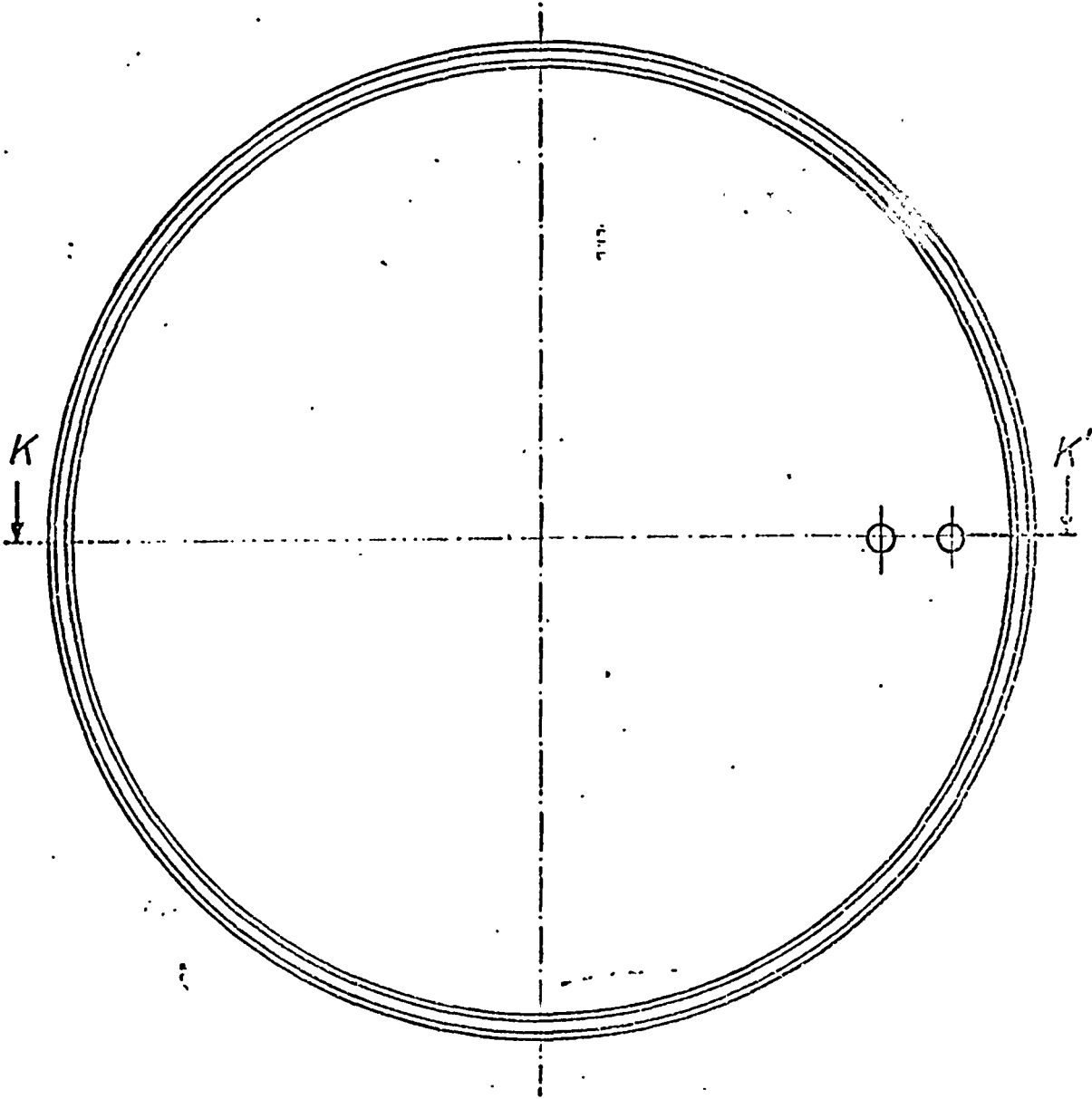
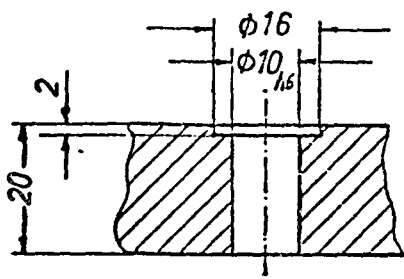
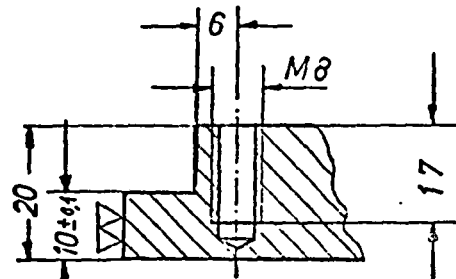


Figure 9: Disc Profile Scale 1:3

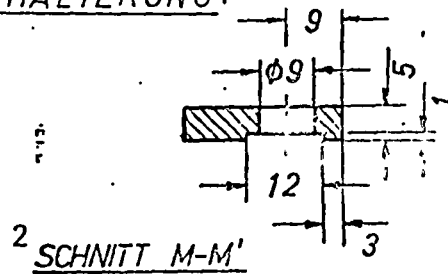
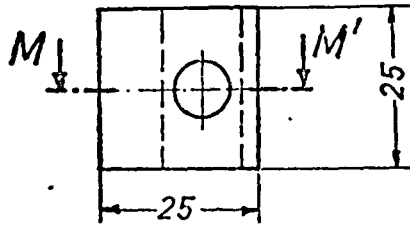


1 EINZELHEIT Z2



2 SCHNITT L-L'

PROFIL-SCHEIBE HALTERUNG<sup>3</sup>



2 SCHNITT M-M'

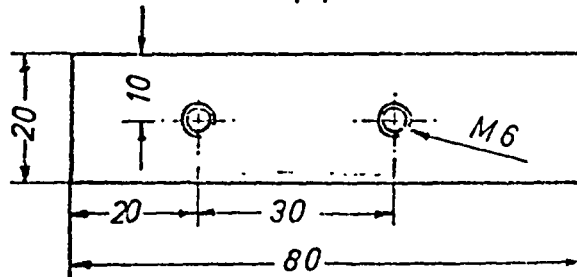
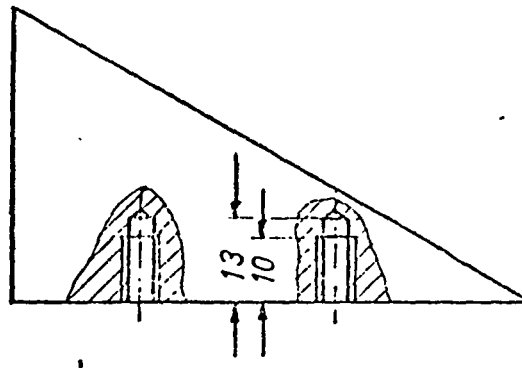
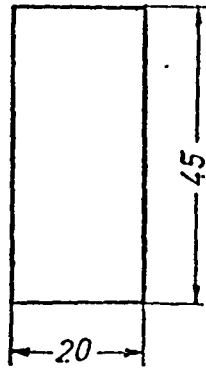
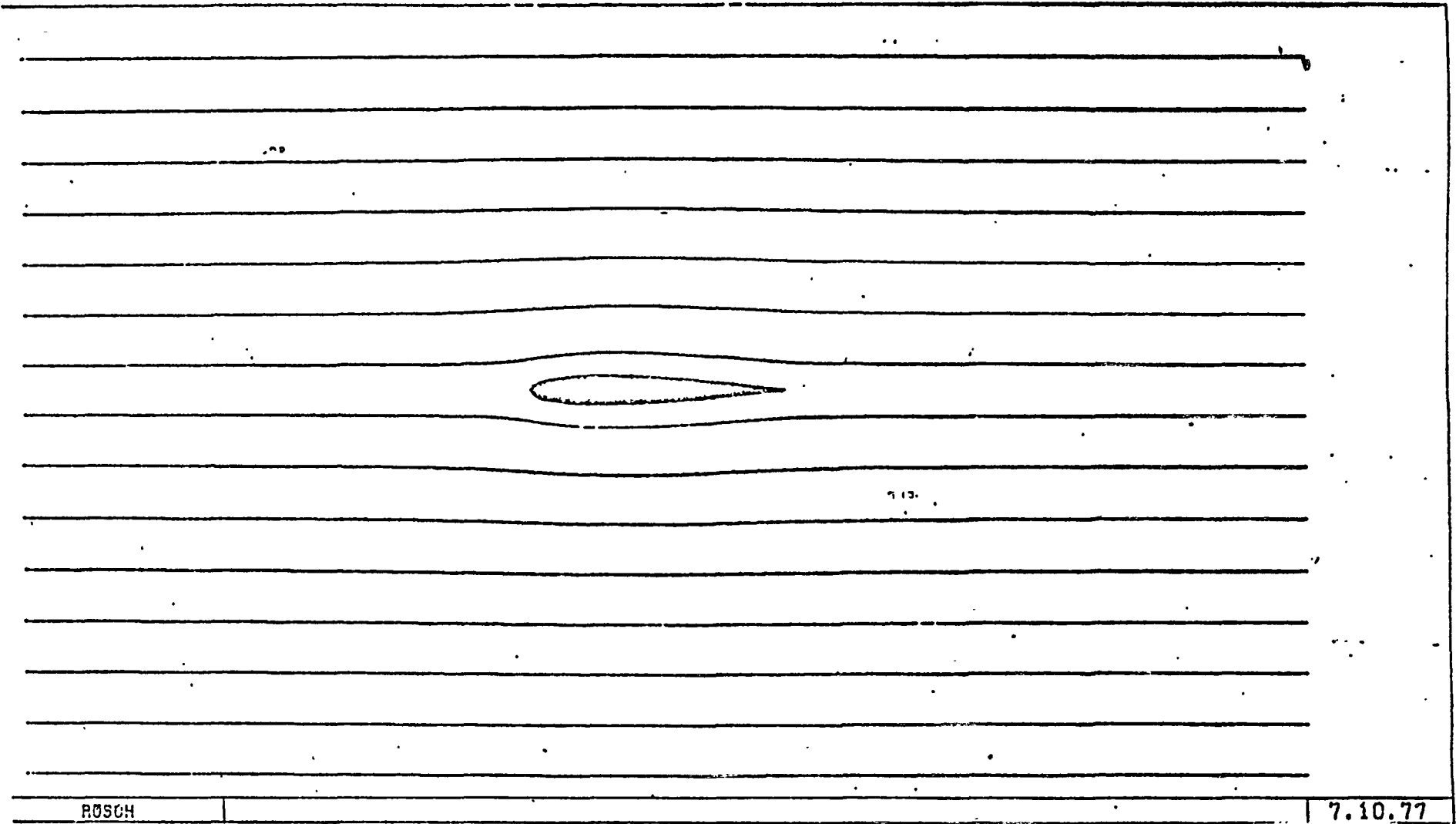


Figure 10: Flange Reinforcement. Scale 1:1

Key: 1-detail 2-cross-section 3-profile of disc mount



RÖSCH

7.10.77

Figure 11: Test with NACA 0012.  $\alpha = 0^\circ$

Flow Lines

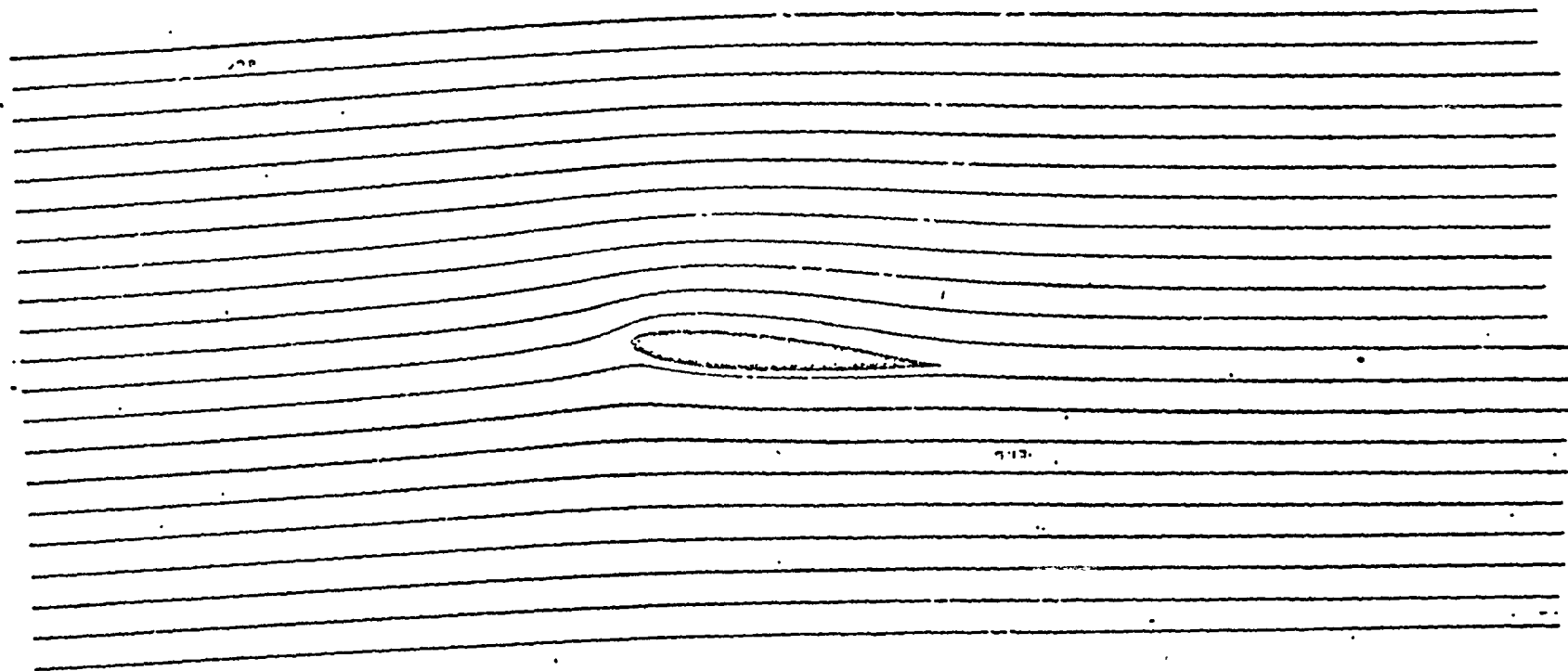


Figure 12: Test with NACA 0012  $\alpha = 6^\circ$  Flow Lines

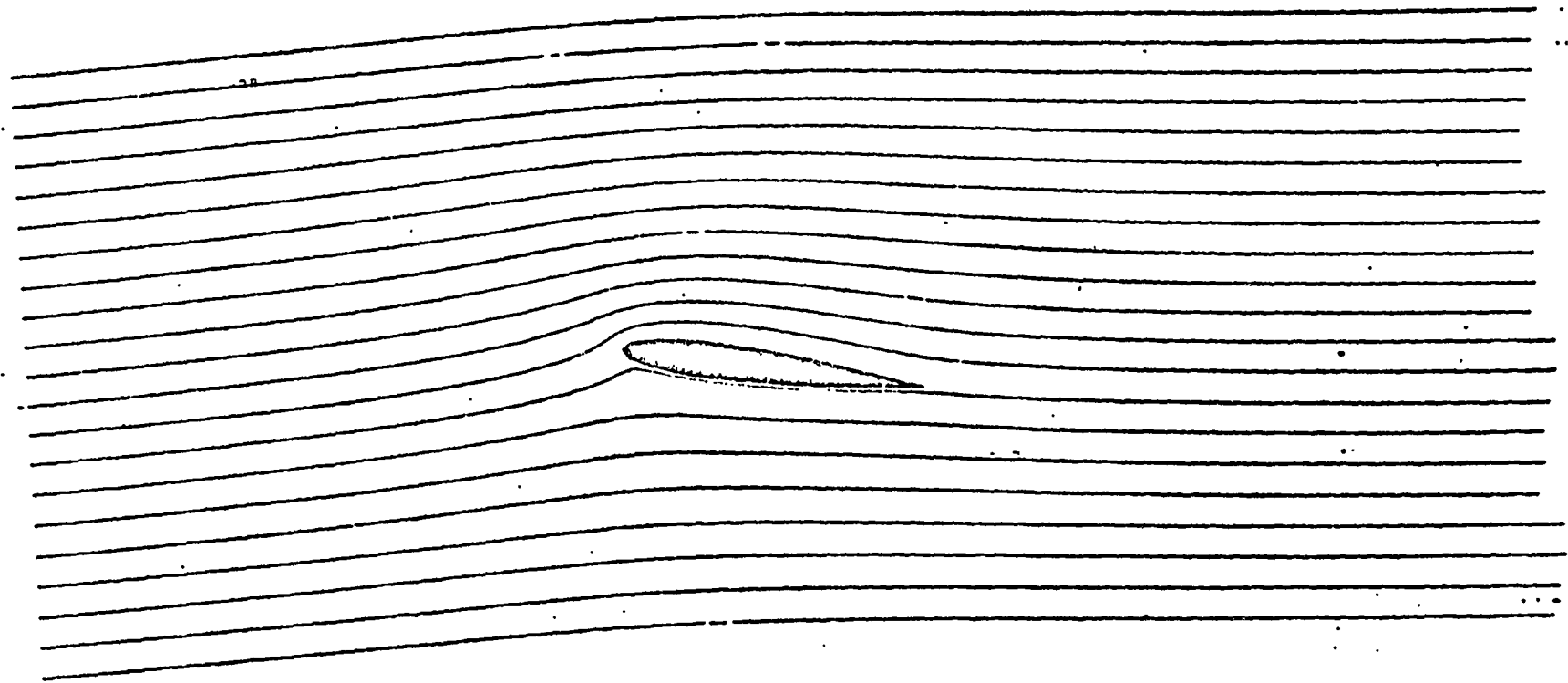
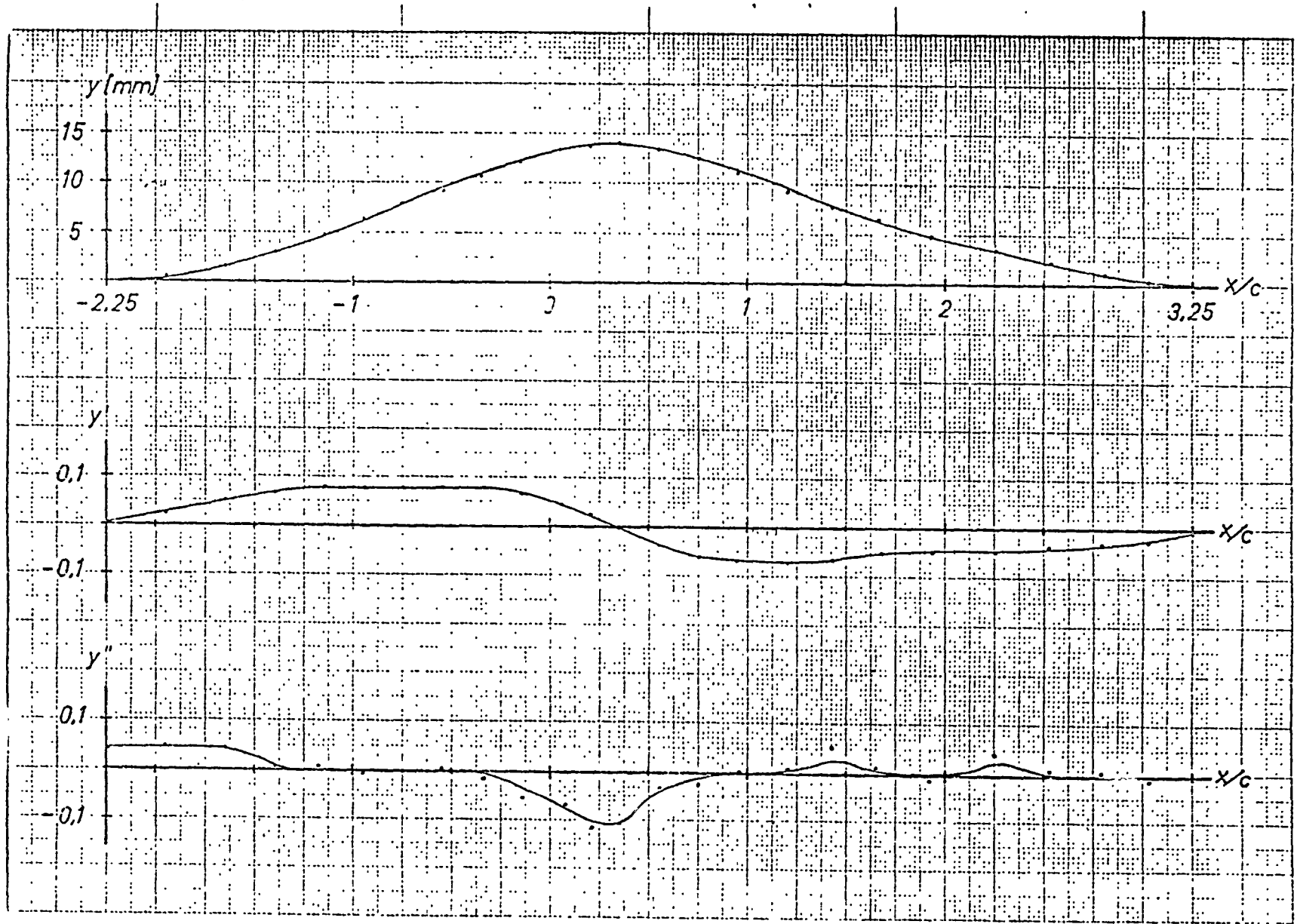


Figure 13. Test with NACA 0012  $\alpha = 10^\circ$  Flow Lines

Figure 14: Wall Contour at  $\alpha = 10^\circ$



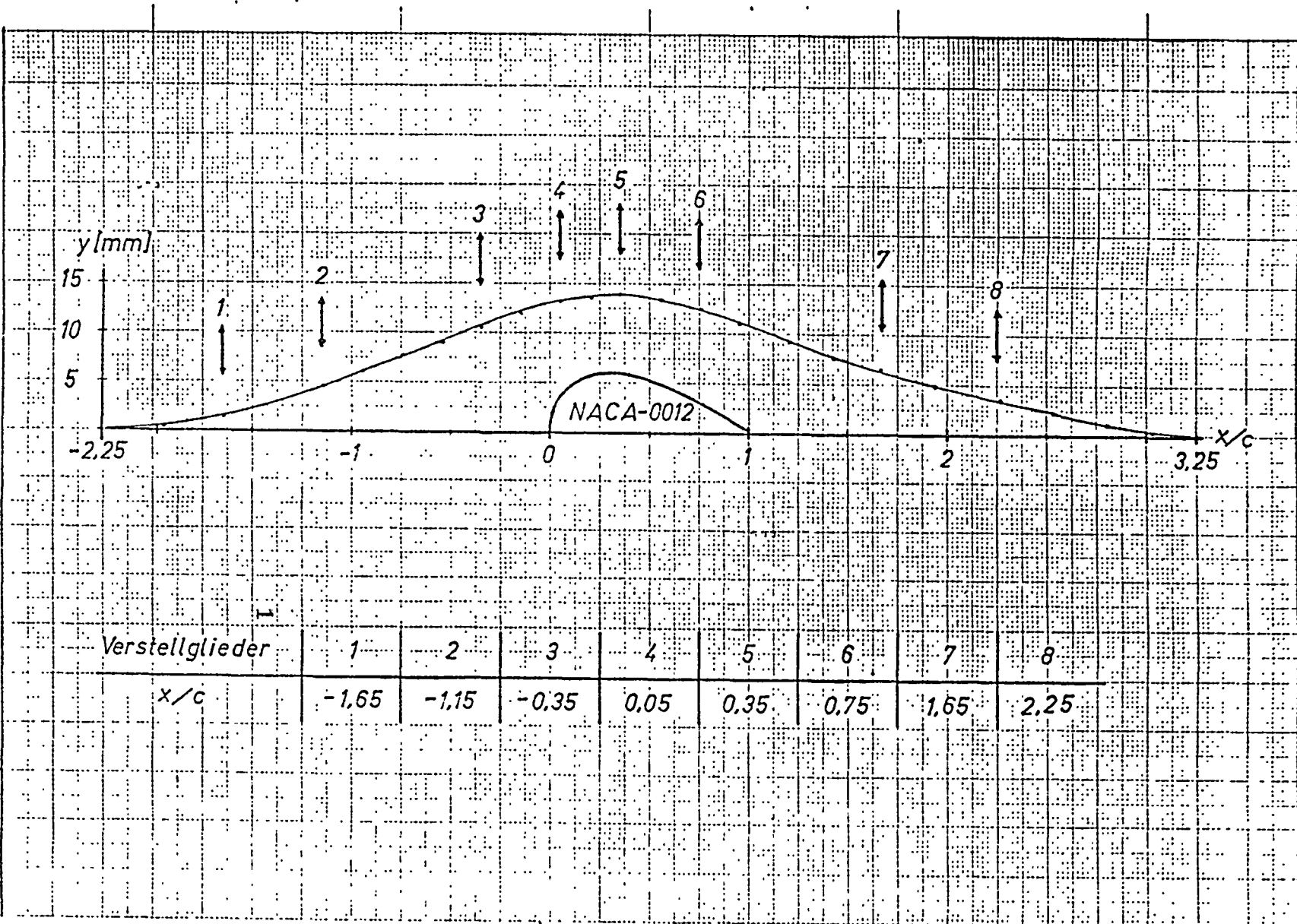


Figure 15: Position of Adjusting Elements

Key: 1-adjusting elements



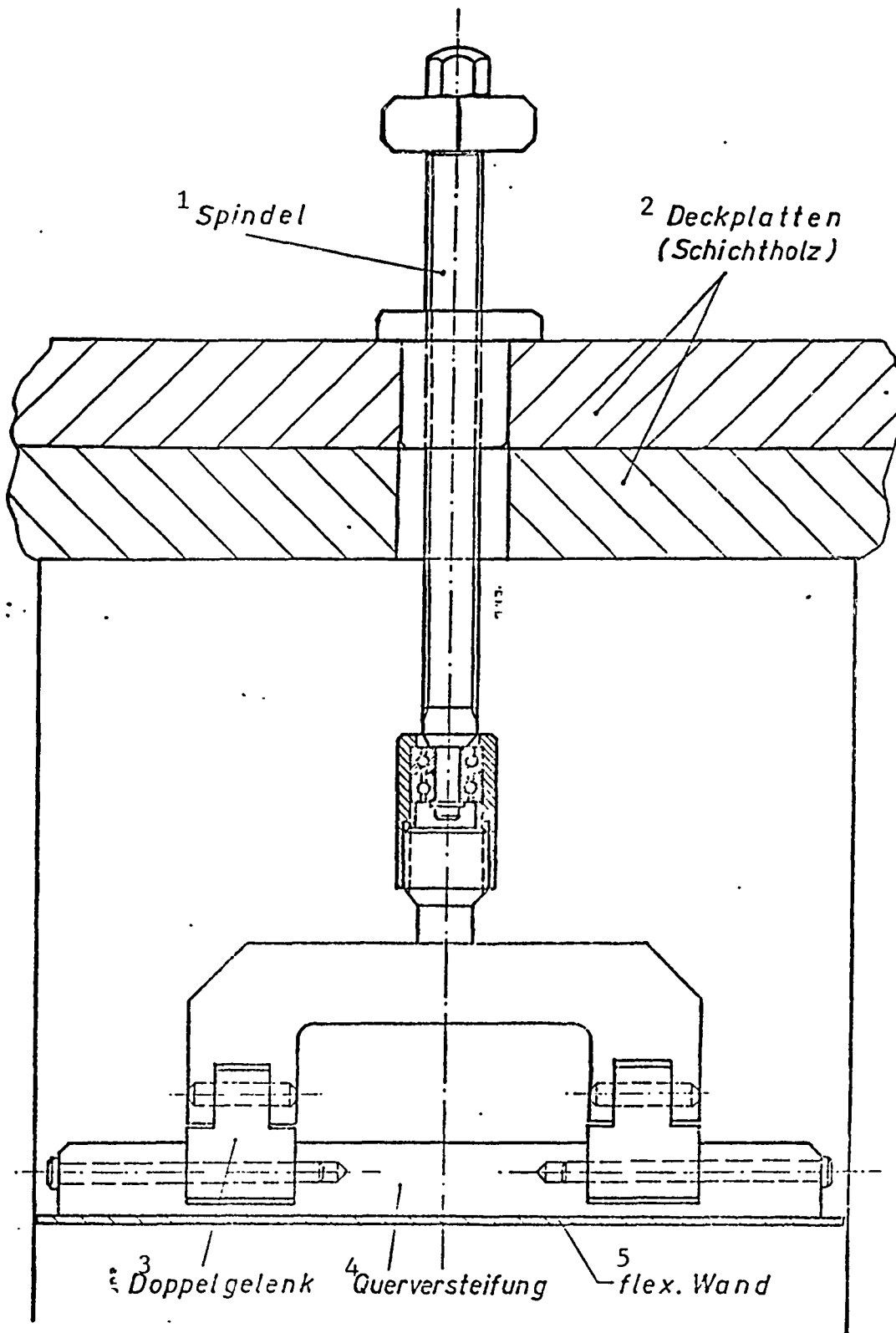


Fig. 16: Adjusting Mechanism

Key: 1-spindle 2-cover plates (plywood) 3-articulated joint  
 4-cross reinforcement 5-flexible wall

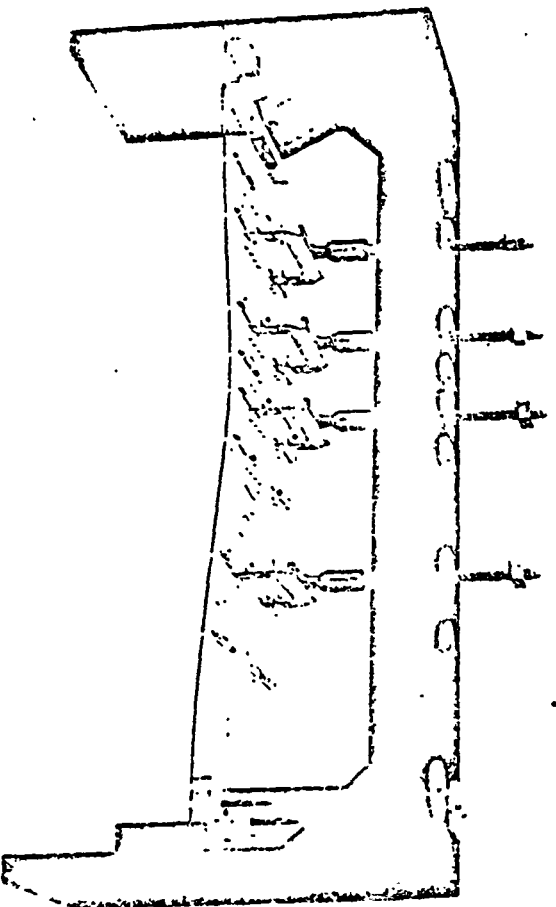


Figure 17:

Test Set-up

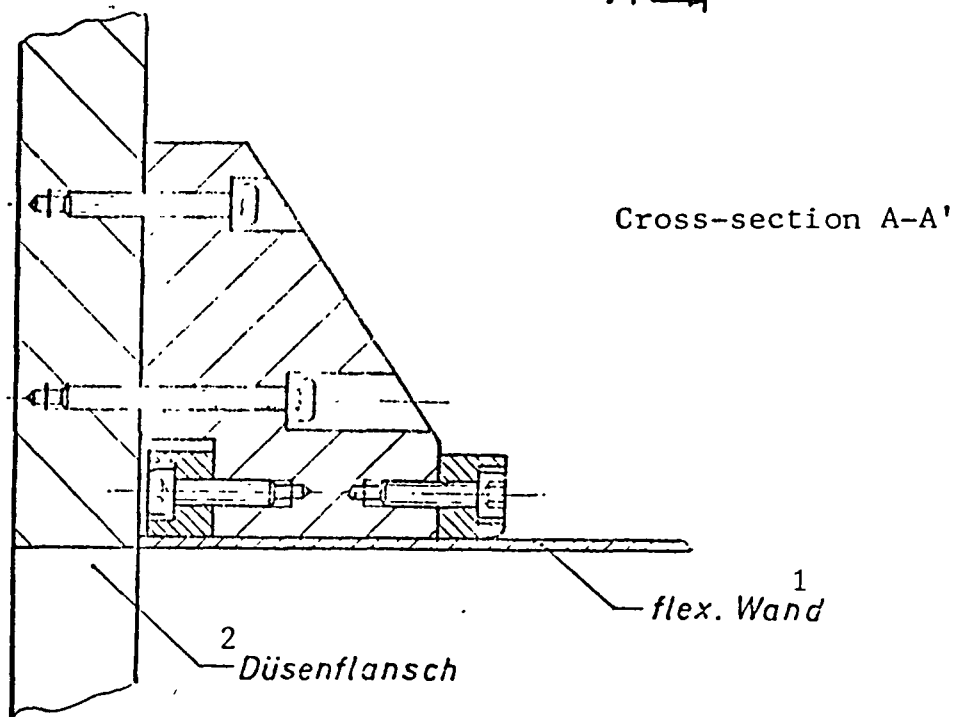
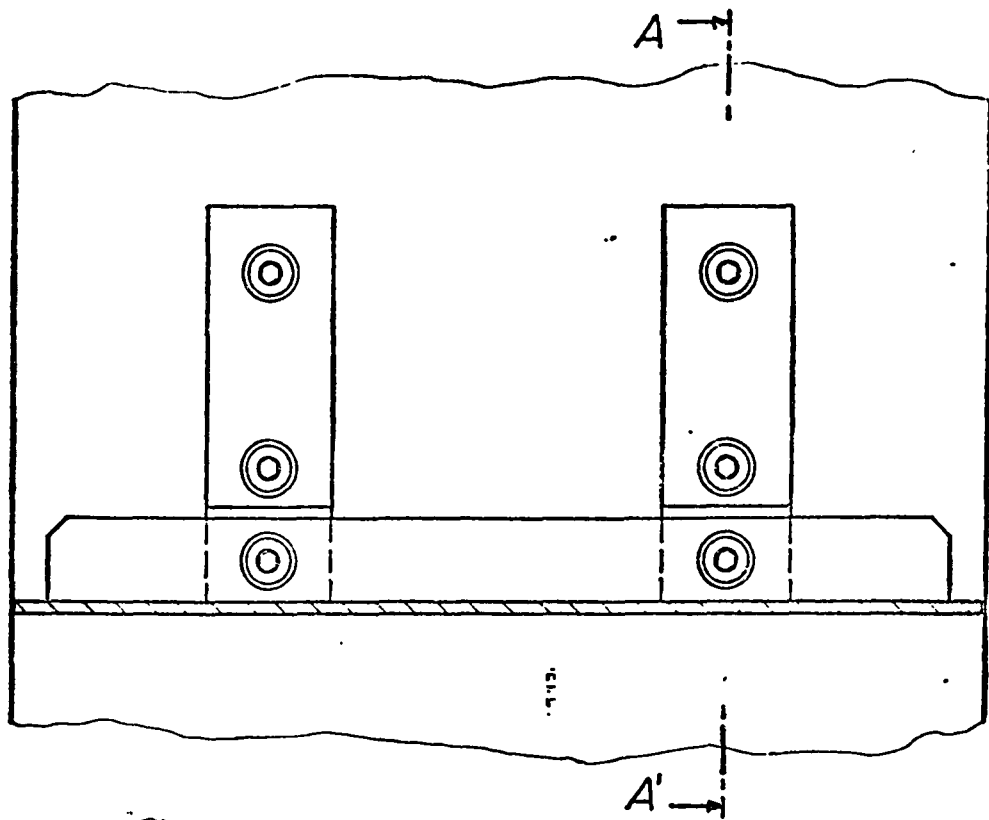


Fig. 18: Front Wall Reinforcement

Key: 1-flexible wall 2-nozzle flange

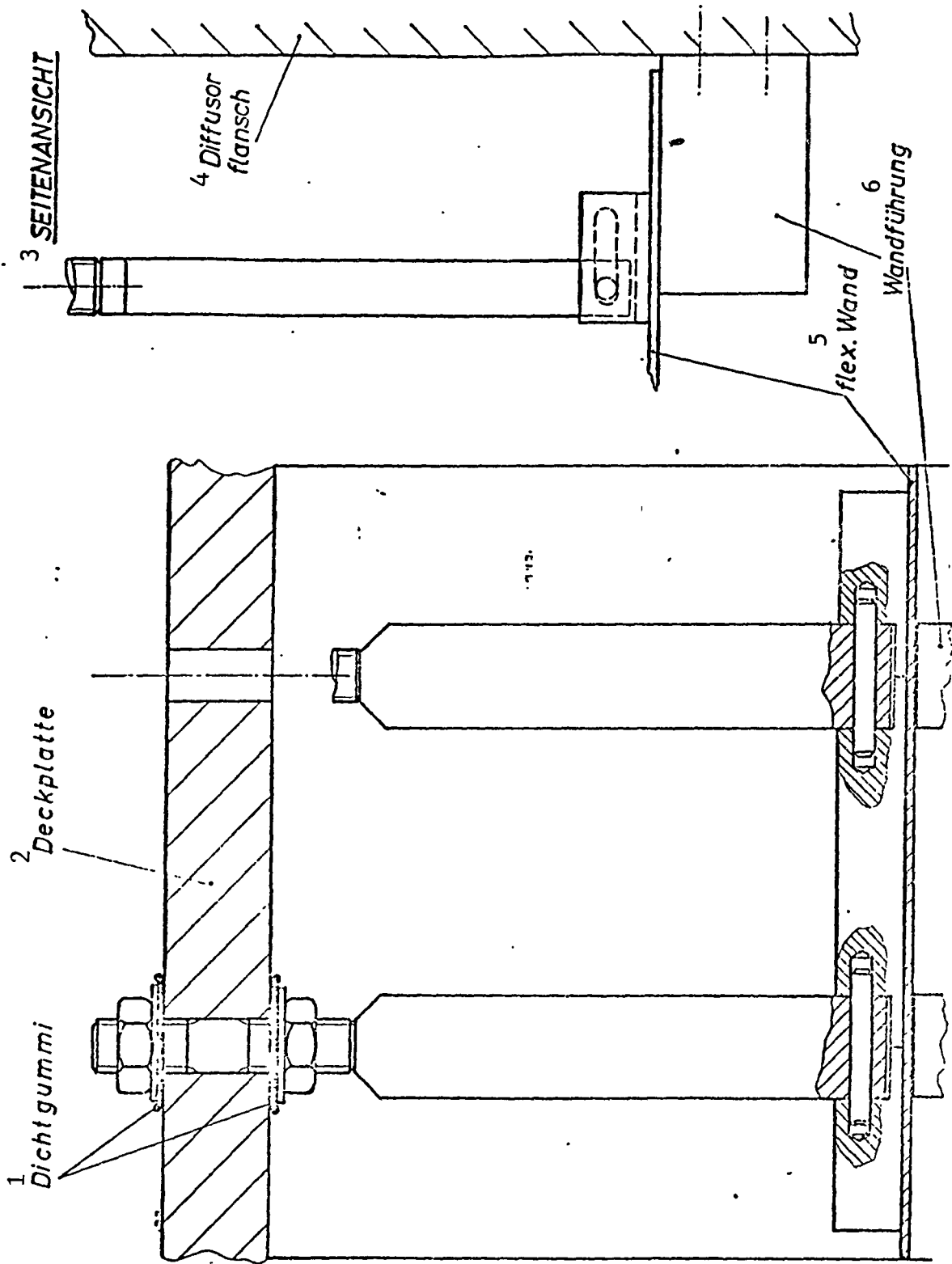
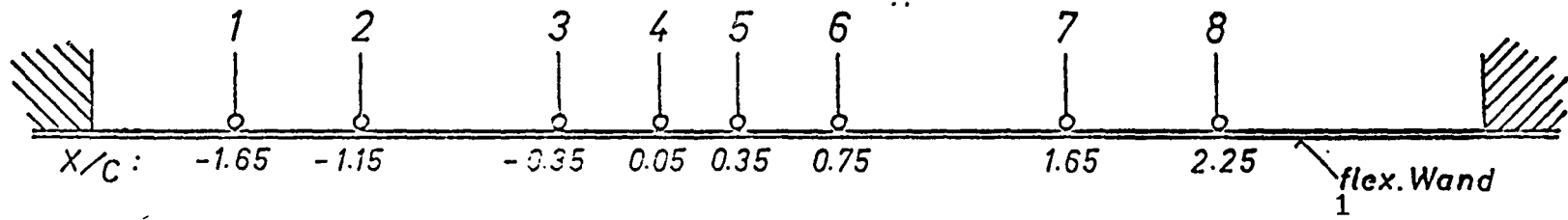


Fig. 19: Rear Wall Attachment

Key: 1-rubber sealant 2-cover plate 3-side vidw 4-diffusor flange  
 5-flexible wall 6-wall lead



2 V E R T E I L U N G

KOMBINATIONEN	A					5	6	7	8
	B	1	2	3	4				
	C		2	3		5		7	
	D			3	4	5	6		
	E		2			5		7	
	F				4	5	6		
	G			3		5	6		
	H		2			5			
	I				4		6		
	J			3			6		
	K					5			

Fig. 20: Distribution of Adjustment Elements  
 Key; 1-flex. wall 2-distribution 3-combinations

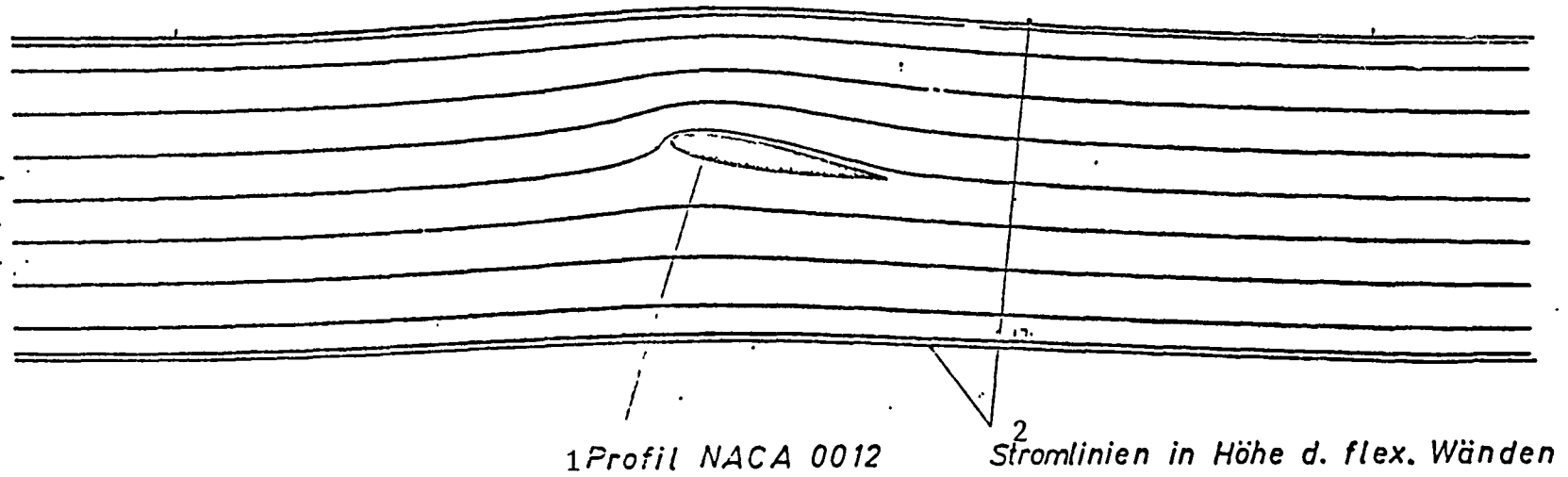


Fig. 21: Test with NACA 0012 in the Windtunnel.  $\alpha = 10.0$

Key: 1-NACA 0012 airfoil 2-flow lines at the level of the flex. walls

Fig. 22: Deviation of Wall Contour (4 adjusting elements)

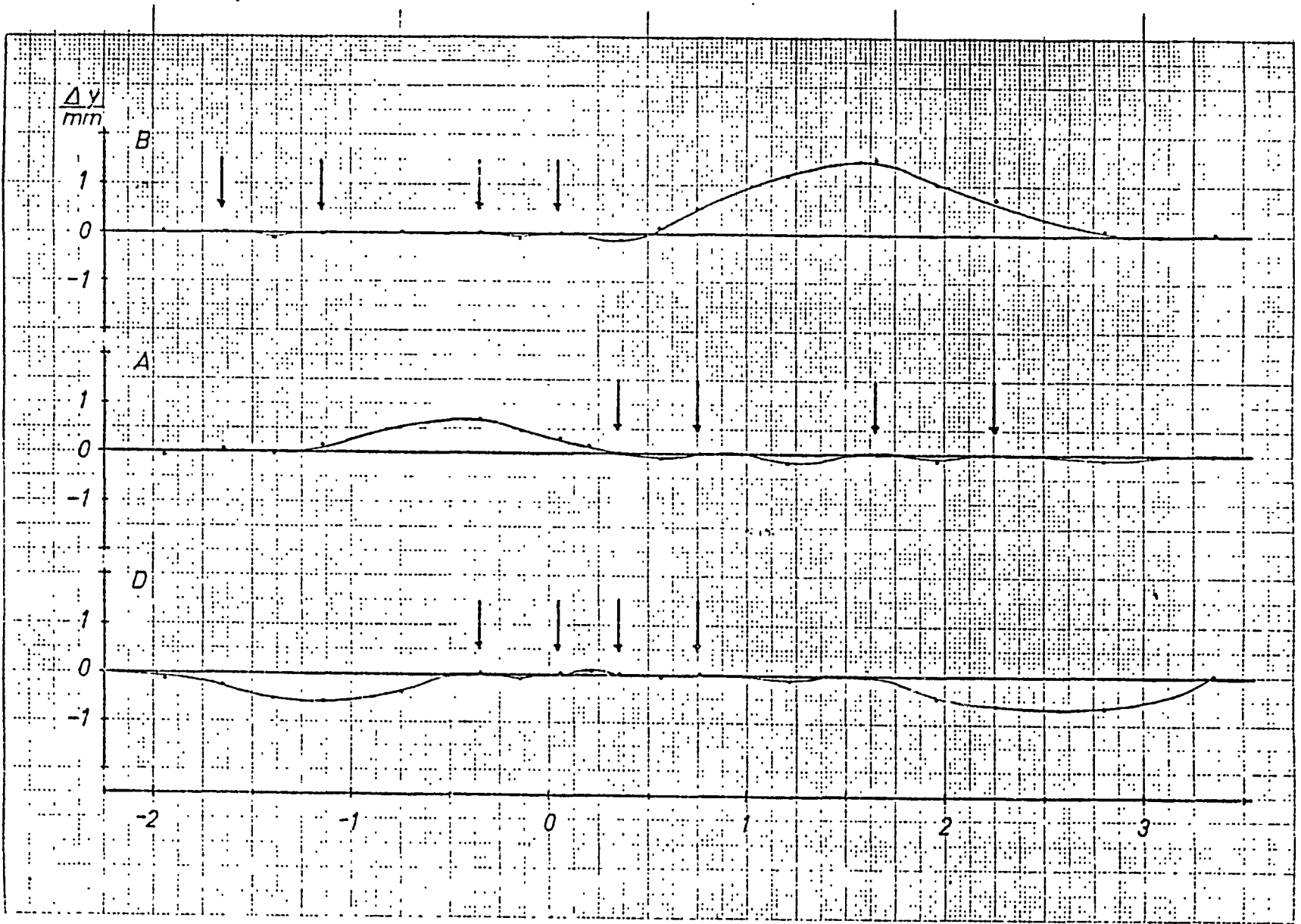


Fig. 23: Deviation of Wall Contour (1 and 4 adjusting elements)

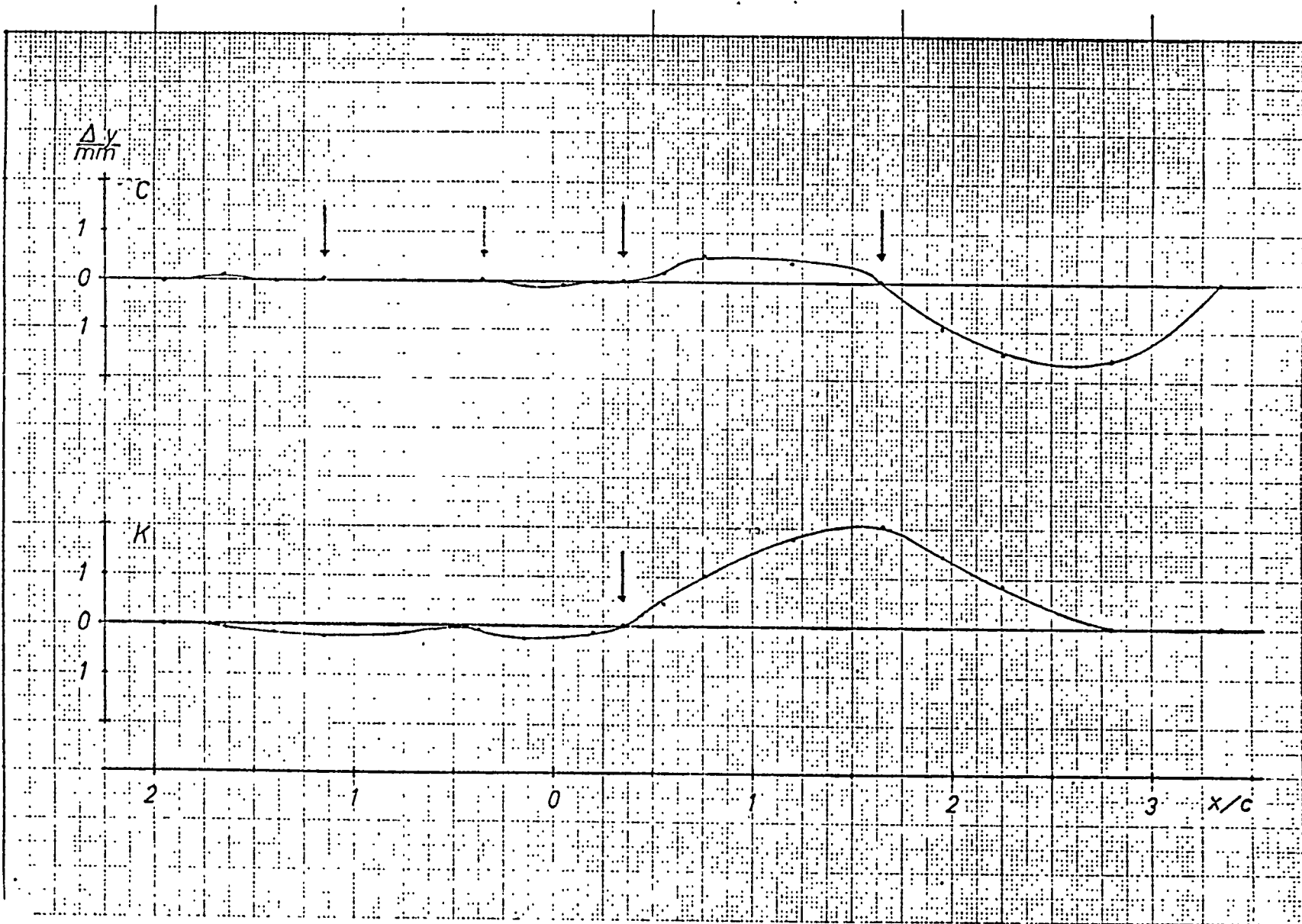




Fig. 24: Deviation of Wall Contour (2 adjusting elements)

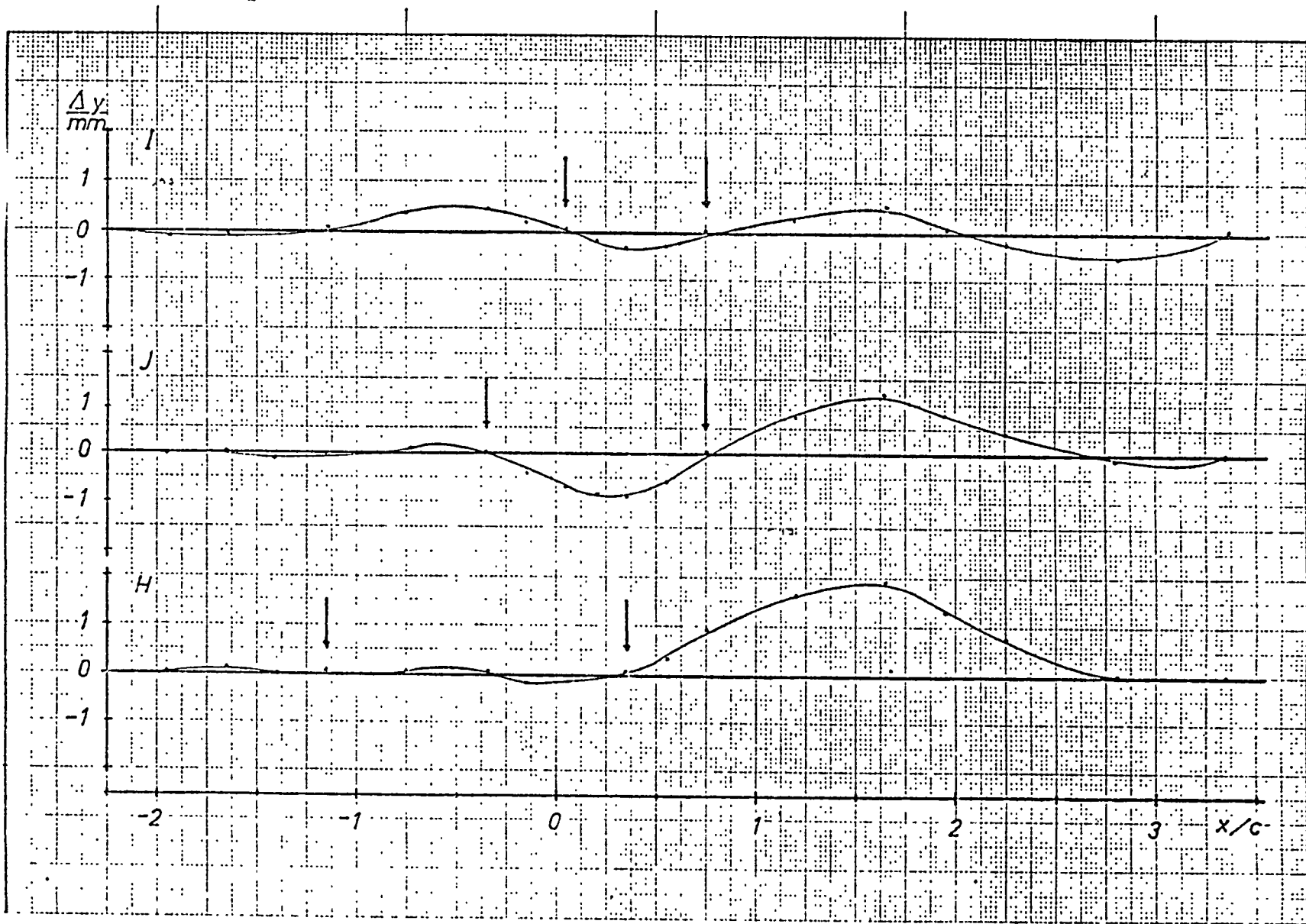
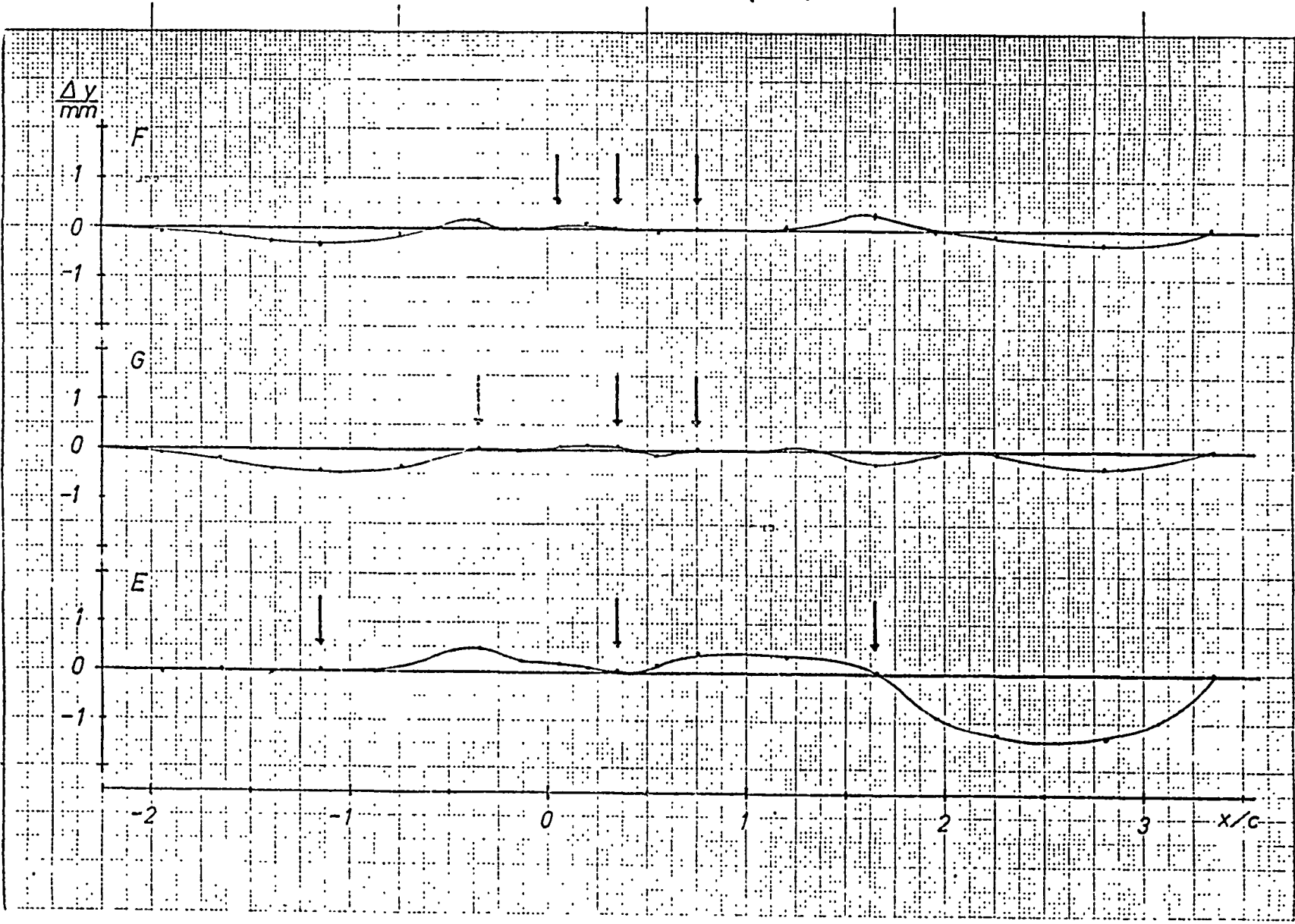


Fig. 25: Deviation of Wall Contour (3 adjusting elements)



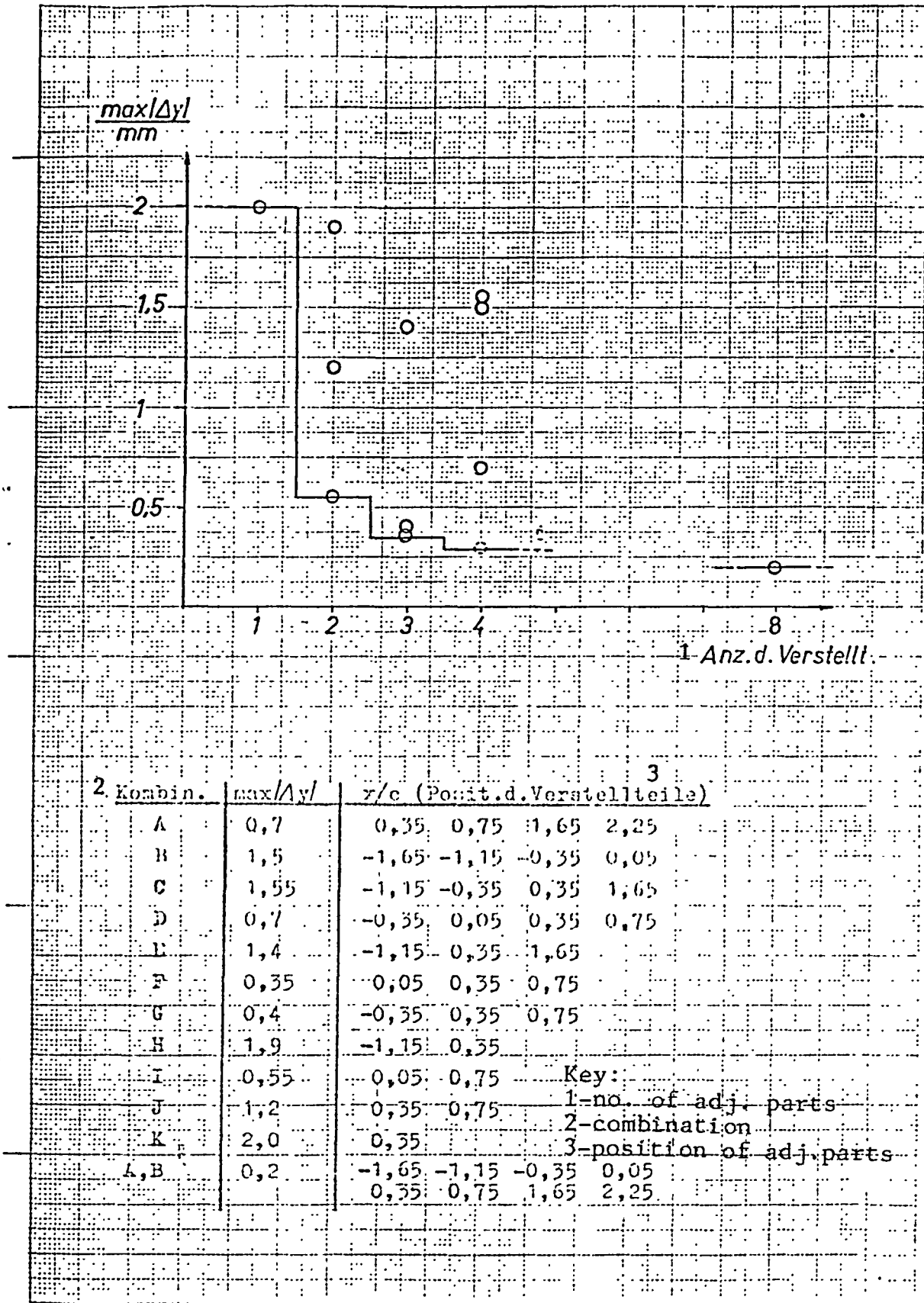


Fig. 26: Wall-adjustment Tolerance

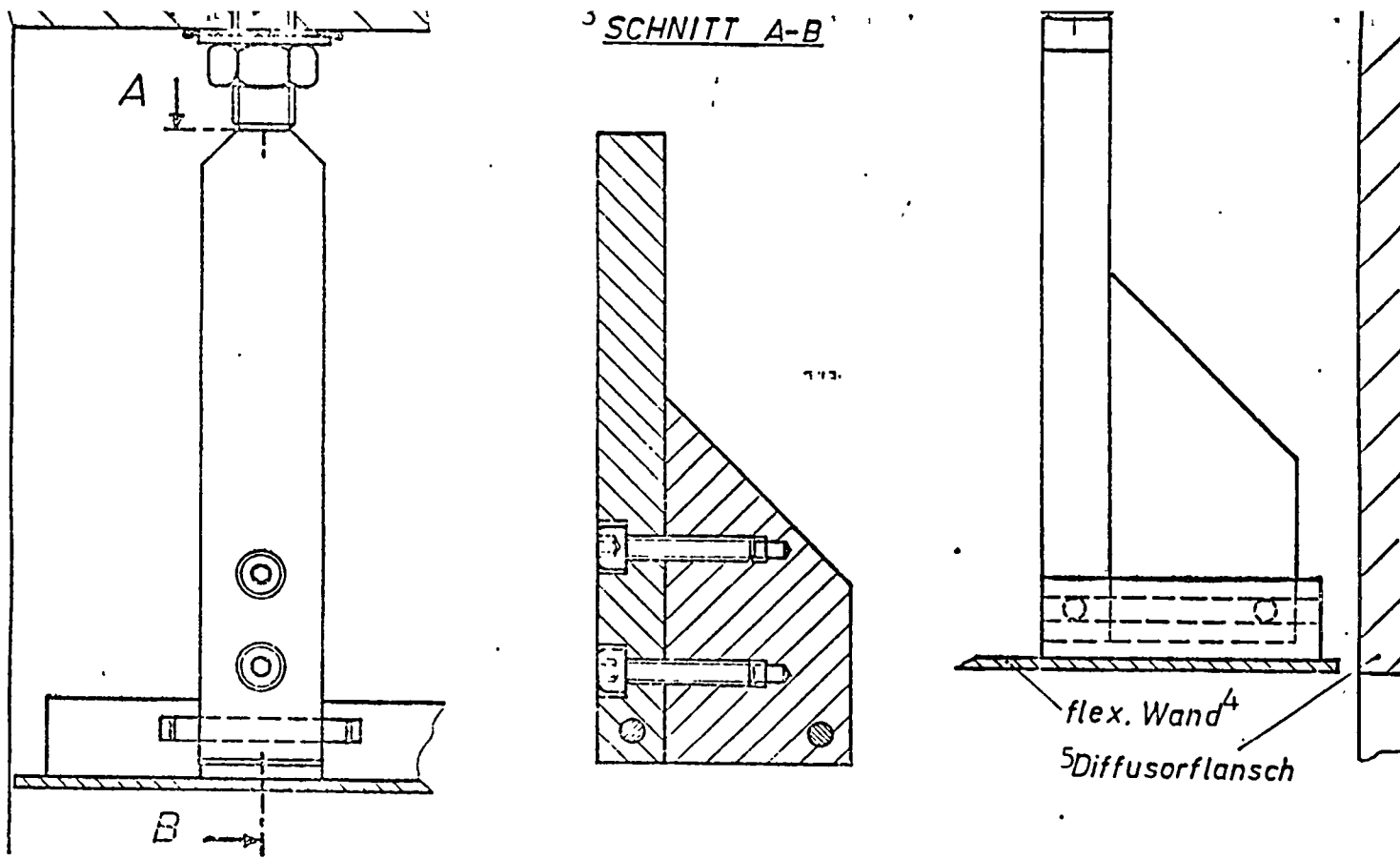


Fig. 27: Rear, Modified Wall Attachment

Key: 1-cover plate 2-side view 3-cross-section 4-flex. wall 5-diffusor flange

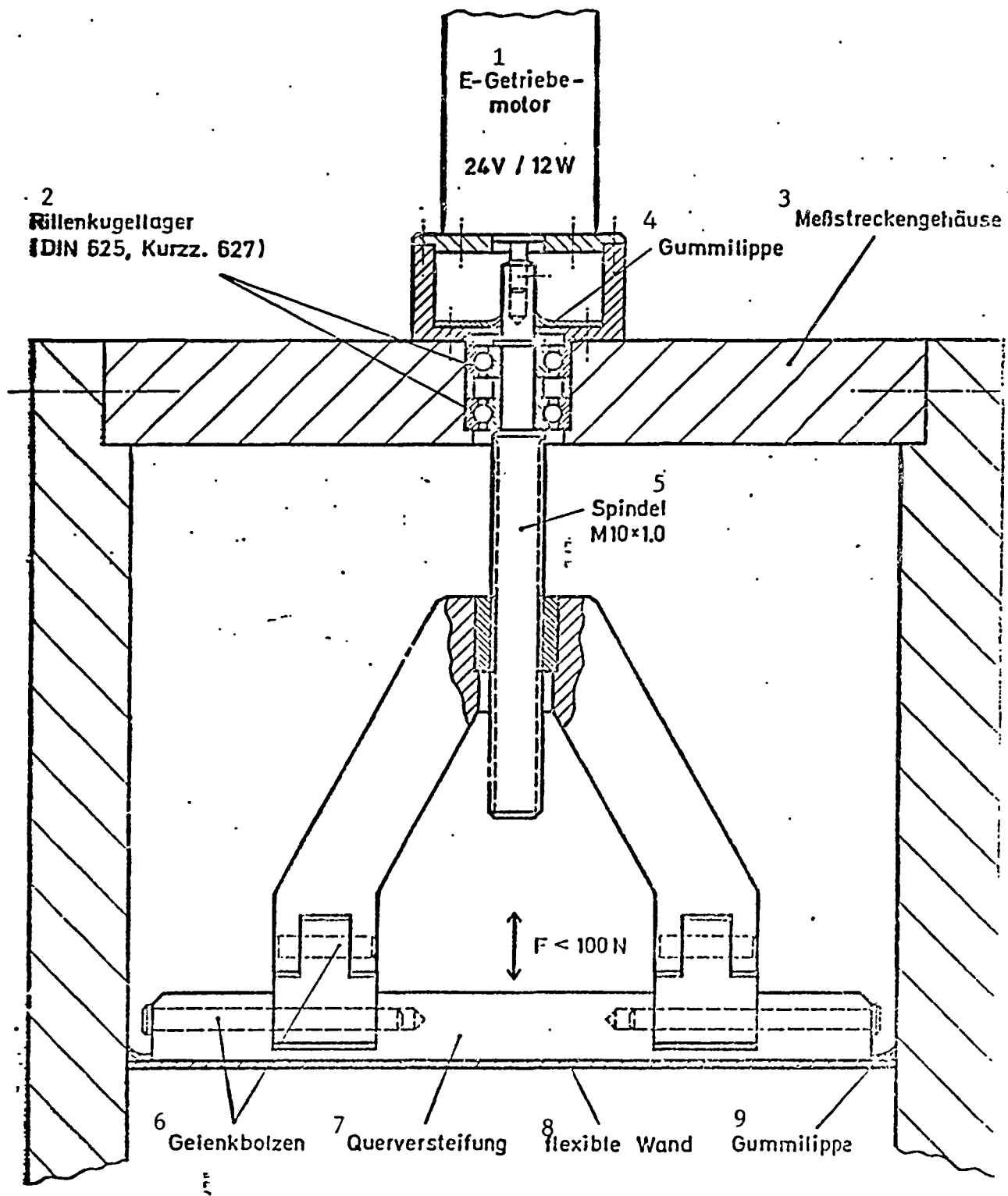


Fig. 28: Electrical Adjusting Mechanism

Key: 1-electrical geared motor 2-grooved ball bearing 3-throat housing 4-rubber lip 5-spindle 6-joint bolt 7-cross-reinforcement 8-flex. wall 9-rubber lip

<sup>a</sup> Stützstelle	X/C	Y
1	-2.3	0.
2	-2.25	0.
3	-1.65	1.5
4	-1.25	4.
5	-0.85	7.
6	-0.45	10.
7	-0.05	12.75
8	0.35	14.
9	0.75	12.5
10	1.15	9.75
11	1.55	7.
12	1.95	5.
13	2.35	3.
14	2.75	1.5
15	3.15	0.25
16	3.25	0.
17	3.3	0.

Table 1: Values input into the Spline Function Program

Key: a-support point

x/c	Wandauslenkung (mm)			max.Diff.
	PC	PMMA	PVC	
-2.25	0.00	0.00	0.00	0.00
-1.95	0.20	0.25	0.30	0.10
-1.65	1.50	1.50	1.55	0.05
-1.40	2.95	2.95	2.95	0.00
-1.15	4.75	4.75	4.75	0.00
-0.75	8.00	8.10	7.95	0.15
-0.35	11.20	11.20	11.10	0.10
-0.15	12.45	12.40	12.35	0.10
0.05	13.40	13.35	13.35	0.05
0.20	13.80	13.80	13.80	0.00
0.35	14.00	14.00	14.00	0.00
0.55	13.60	13.60	13.60	0.00
0.75	12.85	12.80	12.85	0.05
1.20	9.80	9.85	9.85	0.05
1.65	6.50	6.50	6.50	0.00
1.95	4.15	4.25	4.25	0.10
2.25	2.20	2.30	2.25	0.10
2.80	0.10	0.15	0.10	0.05
3.25	0.00	0.00	0.00	0.00

Table 2: Comparison of Wall Contour

Number of adjusting elements: 3

Arrangement: 2-5-7 = E

Key: a-wall deflection

$x/c$	$y$	$y' (10^{-2})$	$y'' (10^{-2})$
-2.25	0.000	0.128	3.831
-1.95	0.389	2.482	4.200
-1.65	1.500	4.946	4.200
-1.4	2.962	6.605	0.673
-1.15	4.730	7.410	0.520
-0.95	6.239	7.618	-1.198
-0.75	7.756	7.534	-0.181
-0.55	9.255	7.461	0.136
-0.35	10.741	7.338	-2.141
-0.15	12.137	6.482	-6.377
0.05	13.275	4.714	-7.663
0.2	13.829	2.543	-12.770
0.35	14.000	-0.394	-11.068
0.55	13.532	-4.018	-3.033
0.75	12.500	-6.034	-3.033
0.96	11.142	-6.991	-0.140
1.2	9.383	-7.340	0.818
1.43	7.786	-6.675	5.567
1.65	6.451	-5.188	1.174
1.95	5.000	-4.905	-1.636
2.25	3.476	-4.942	4.657
2.53	2.277	-3.777	0.997
2.8	1.342	-3.136	0.339
3.08	0.491	-3.159	-2.055
3.25	0.000	-0.844	25.322

Table to fig. 14: Values computed with the Spline Function Program



a Wandauslenkung (mm)					
x/c	SOLL <sup>b</sup>	D		K	
		c <sub>IST</sub>	diff.	c <sub>IST</sub>	diff.
-2.25	0.00	0.00	0.00	0.00	0.00
-1.95	0.25	0.10	-0.15	0.25	0.00
-1.65	1.50	1.20	-0.30	1.45	-0.05
-1.40	3.00	2.45	-0.55	2.80	-0.20
-1.15	4.75	4.15	-0.60	4.50	-0.25
-0.75	7.75	7.35	-0.40	7.60	-0.15
-0.35	10.75	10.75	0.00	10.65	-0.10
-0.15	12.25	12.15	-0.10	11.95	-0.30
0.05	13.25	13.25	0.00	13.00	-0.25
0.20	13.75	13.80	0.05	13.60	-0.15
0.35	14.00	14.00	0.00	14.00	0.00
0.55	13.50	13.45	-0.05	13.90	0.40
0.75	12.50	12.50	0.00	13.50	1.00
1.20	9.50	9.35	-0.05	11.25	1.75
1.65	6.50	6.45	-0.05	8.50	2.00
1.95	5.00	4.50	-0.50	6.40	1.40
2.25	3.50	2.85	-0.65	4.30	0.80
2.80	1.50	0.80	-0.70	1.50	0.00
3.25	0.00	0.00	0.00	0.00	0.00

Table to figures 22, 23: Deviation of Wall Contour

Wall material: PC

Number of adjusting elements: 4 and 1

Arrangement: 3-4-5-6 = D

Key: a-wall deflection    b-theoretical    c-actual

a Wandauslenkung (mm)							
x/c	SOLL <sup>b</sup>	A		B		C	
		c <sub>IST</sub>	diff.	c <sub>IST</sub>	diff.	c <sub>IST</sub>	diff.
-2.25	0.00	0.00	0.00	0.00	0.00	0.00	0.00
-1.95	0.25	0.20	-0.05	0.25	0.00	0.20	-0.05
-1.65	1.50	1.55	0.05	1.50	0.00	1.55	0.05
-1.40	3.00	3.00	0.00	2.90	-0.10	2.95	-0.05
-1.15	4.75	4.9	0.15	4.75	0.00	4.75	0.00
-0.75	7.75	8.25	0.50	7.75	0.00	7.75	0.00
-0.35	10.75	11.45	0.70	10.75	0.00	10.75	0.00
-0.15	12.25	12.70	0.45	12.15	-0.10	12.10	-0.15
0.05	13.25	13.55	0.30	13.25	0.00	13.15	-0.10
0.20	13.75	13.90	0.15	13.65	-0.10	13.70	-0.05
0.35	14.00	14.00	0.00	13.85	-0.15	14.00	0.00
0.55	13.50	13.40	-0.10	13.60	0.10	13.65	0.15
0.75	12.50	12.50	0.00	13.00	0.50	13.00	0.50
1.20	9.50	9.30	-0.20	10.65	1.15	9.85	0.35
1.65	6.50	6.50	0.00	8.00	1.50	6.50	0.00
1.95	5.00	4.85	-0.15	6.00	1.00	4.00	-1.00
2.25	3.50	3.50	0.00	4.20	0.70	2.00	-1.50
2.80	1.50	1.35	-0.15	1.55	0.05	-0.05	-1.55
3.25	0.00	0.00	0.00	0.00	0.00	0.00	0.00

Table to figures 22, 23: Deviation of Wall Contour

Wall material: PC

Number of adjusting elements: 4

Arrangement: 5-6-7-8 = A; 1-2-3-4 = B; 2-3-5-7 = C

Key :a-wall deflection b-theoretical c-actual

x/c	<sup>a</sup> Wandauslenkung (mm)						
	SOLL <sup>b</sup>	<sup>c</sup> IST	<sup>H</sup> diff.	<sup>c</sup> IST	<sup>I</sup> diff.	<sup>c</sup> IST	<sup>J</sup> diff.
-2.25	0.00	0.00	0.00	0.00	0.00	0.00	0.00
-1.95	0.25	0.25	0.00	0.15	-0.10	0.20	-0.05
-1.65	1.50	1.55	0.05	1.45	-0.05	1.50	0.00
-1.40	3.00	3.00	0.00	2.90	-0.10	2.90	-0.10
-1.15	4.75	4.75	0.00	4.80	0.05	4.70	-0.05
-0.75	7.75	7.75	0.00	8.10	0.35	7.80	0.05
-0.35	10.75	10.80	0.05	11.20	0.45	10.75	0.00
-0.15	12.25	12.05	-0.20	12.40	0.15	11.80	-0.45
0.05	13.25	13.10	-0.15	13.25	0.00	12.55	-0.70
0.20	13.75	13.70	-0.05	13.55	-0.20	12.90	-0.85
0.35	14.00	14.00	0.00	13.65	-0.35	13.10	-0.90
0.55	13.50	13.80	0.30	13.20	-0.30	12.90	-0.60
0.75	12.50	13.40	0.90	12.50	0.00	12.50	0.00
1.20	9.50	11.10	1.60	9.75	0.25	10.25	0.75
1.65	6.50	8.40	1.90	7.00	0.50	7.70	1.20
1.95	5.00	6.25	1.25	5.00	0.00	5.75	0.75
2.25	3.50	4.25	0.75	3.25	-0.25	3.90	0.40
2.80	1.50	1.50	0.00	0.95	-0.55	1.35	-0.15
3.25	0.00	0.00	0.00	0.00	0.00	0.00	0.00

Table to fig. 24: Deviation of Wall Contour

Wall material: PC

Number of adjusting elements: 2

Arrangement: 2-5 = H; 4-6 = I; 3-6 = J

Key: a-wall deflection b-theoretical c-actual

x/c	a Wandauslenkung (mm)						
	b SOLL	c IST	E diff.	c IST	F diff.	c IST	G diff.
-2.25	0.00	0.00	0.00	0.00	0.00	0.00	0.00
-1.95	0.25	0.20	-0.05	0.15	-0.10	0.15	-0.10
-1.65	1.50	1.50	0.00	1.35	-0.15	1.30	-0.20
-1.40	3.00	2.95	-0.05	2.70	-0.30	2.60	-0.40
-1.15	4.75	4.75	0.00	4.45	-0.35	4.30	-0.45
-0.75	7.75	8.00	0.05	7.65	-0.10	7.40	-0.35
-0.35	10.75	11.20	0.45	10.90	0.15	10.75	0.00
-0.15	12.25	12.45	0.20	12.20	-0.05	12.20	-0.05
0.05	13.25	13.40	0.15	13.25	0.00	13.30	0.05
0.20	13.75	13.80	0.05	13.80	0.05	13.80	0.05
0.35	14.00	14.00	0.00	14.00	0.00	14.00	0.00
0.55	13.50	13.60	0.10	13.45	-0.05	13.40	-0.10
0.75	12.50	12.85	0.35	12.50	0.00	12.50	0.00
1.20	9.50	9.80	0.30	9.50	0.00	9.50	0.00
1.65	6.50	6.50	0.00	6.80	0.30	6.80	-0.30
1.95	5.00	4.15	-0.85	4.95	-0.05	4.90	-0.10
2.25	3.50	2.20	-1.30	3.35	-0.15	3.40	-0.10
2.80	1.50	0.10	-1.40	1.15	-0.30	1.10	-0.40
3.25	0.00	0.00	0.00	0.00	0.00	0.00	0.00

Table to fig. 25: Deviation of Wall Contour

Wall material: PC

Number of adjusting elements: 3

Arrangement: 2-5-7 = E; 4-5-6 = F; 3-5-6 = G

Key: a-wall deflection b-theoretical c-actual

**End of Document**